Volume 9, Issue 16 – January – June – 2023

ECORFAN

Journal-Democratic Republic of Congo

ISSN-On line 2414-4924

ECORFAN®

ECORFAN Journal - Democratic Republic of Congo, Volume 9, Issue 16, January – June 2023, is a journal edited semestral by ECORFAN. 6593 Kinshasa 31Rép.DémocratiqueduCongo.WEB:www.ecorfan.org/DemocraticRepublicofCongo/,journal@ec orfan.org. Editor in Chief: ILUNGA-MBUYAMBA, Elisée. MsC. ISSN On line: 2414-4924. Responsible for the latest update of this number ECORFAN Computer Unit. ESCAMILLA-BOUCHÁN, Imelda. PhD, LUNA-SOTO, Vladimir. PhD, 6593 Kinshasa 31 Rép. Démocratique du Congo, last updated June 30, 2023.

ECORFAN-Democratic Republic of Congo

Definition of Journal

Scientific Objectives

Support the international scientific community in its written production Science, Technology and Innovation in the Field of Physical Sciences Mathematics and Earth sciences, in Subdisciplines of image and signal processing, control-digital system-artificial, intelligence-fuzzy, logic-mathematical, modeling-computational, mathematics-computer, science.

ECORFAN-Mexico SC is a Scientific and Technological Company in contribution to the Human Resource training focused on the continuity in the critical analysis of International Research and is attached to CONAHCYT-RENIECYT number 1702902, its commitment is to disseminate research and contributions of the International Scientific Community, academic institutions, agencies and entities of the public and private sectors and contribute to the linking of researchers who carry out scientific activities, technological developments and training of specialized human resources with governments, companies and social organizations.

Encourage the interlocution of the International Scientific Community with other Study Centers in Mexico and abroad and promote a wide incorporation of academics, specialists and researchers to the publication in Science Structures of Autonomous Universities - State Public Universities - Federal IES - Polytechnic Universities - Technological Universities - Federal Technological Institutes - Normal Schools - Decentralized Technological Institutes - Intercultural Universities - S & T Councils - CONAHCYT Research Centers.

Scope, Coverage and Audience

ECORFAN-Democratic Republic of Congo is a Journal edited by ECORFAN-Mexico S.C in its Holding with repository in Democratic Republic of Congo, is a scientific publication arbitrated and indexed with semester periods. It supports a wide range of contents that are evaluated by academic peers by the Double-Blind method, around subjects related to the theory and practice of image and signal processing, control-digital system-artificial, intelligence-fuzzy, logic-mathematical, modeling-computational, mathematics-computer, science with diverse approaches and perspectives , That contribute to the diffusion of the development of Science Technology and Innovation that allow the arguments related to the decision making and influence in the formulation of international policies in the Field of Physical Sciences Mathematics and Earth sciences. The editorial horizon of ECORFAN-Mexico® extends beyond the academy and integrates other segments of research and analysis outside the scope, as long as they meet the requirements of rigorous argumentative and scientific, as well as addressing issues of general and current interest of the International Scientific Society.

Editorial Board

Arbitration Committee

Assignment of Rights

The sending of an Article to ECORFAN-Democratic Republic of Congo emanates the commitment of the author not to submit it simultaneously to the consideration of other series publications for it must complement the Originality Format for its Article.

The authors sign the Authorization Format for their Article to be disseminated by means that ECORFAN-Mexico, S.C. In its Holding Democratic Republic of Congo considers pertinent for disclosure and diffusion of its Article its Rights of Work.

Declaration of Authorship

Indicate the Name of Author and Coauthors at most in the participation of the Article and indicate in extensive the Institutional Affiliation indicating the Department.

Identify the Name of Author and Coauthors at most with the CVU Scholarship Number-PNPC or SNI-CONAHCYT- Indicating the Researcher Level and their Google Scholar Profile to verify their Citation Level and H index.

Identify the Name of Author and Coauthors at most in the Science and Technology Profiles widely accepted by the International Scientific Community ORC ID - Researcher ID Thomson - arXiv Author ID - PubMed Author ID - Open ID respectively.

Indicate the contact for correspondence to the Author (Mail and Telephone) and indicate the Researcher who contributes as the first Author of the Article.

Plagiarism Detection

All Articles will be tested by plagiarism software PLAGSCAN if a plagiarism level is detected Positive will not be sent to arbitration and will be rescinded of the reception of the Article notifying the Authors responsible, claiming that academic plagiarism is criminalized in the Penal Code.

Arbitration Process

All Articles will be evaluated by academic peers by the Double Blind method, the Arbitration Approval is a requirement for the Editorial Board to make a final decision that will be final in all cases. MARVID® is a derivative brand of ECORFAN® specialized in providing the expert evaluators all of them with Doctorate degree and distinction of International Researchers in the respective Councils of Science and Technology the counterpart of CONAHCYT for the chapters of America-Europe-Asia-Africa and Oceania. The identification of the authorship should only appear on a first removable page, in order to ensure that the Arbitration process is anonymous and covers the following stages: Identification of the Journal with its author occupation rate - Identification of Authors and Coauthors - Detection of plagiarism PLAGSCAN - Review of Formats of Authorization and Originality-Allocation to the Editorial Board- Allocation of the pair of Expert Arbitrators-Notification of Arbitration - Declaration of observations to the Author-Verification of Article Modified for Editing-Publication.

Instructions for Scientific, Technological and Innovation Publication

Knowledge Area

The works must be unpublished and refer to topics of Image and signal processing, control-digital system-artificial, intelligence-fuzzy, logic-mathematical, modeling-computational, mathematics-computer, science and other topics related to Physical Sciences Mathematics and Earth sciences.

Presentation of the Content

In the first article we present, *Gunshot detection neural network implemented on a low-cost microcontroller* by RODRÍGUEZ-PONCE, Rafael, with adscription in the Universidad Politécnica de Guanajuato, as the next article we present, *Transfer Learning to improve the Diagnosis of Type 2 Diabetes Mellitus (T2D)* by CUTIÉ-TORRES, Carmen, LUNA-ROSAS, Francisco Javier, LUNA-MEDINA, Marisol and DUNAY-ACEVEDO, Cesar, with adscription in the Instituto Tecnológico de Aguascalientes and Universidad Autónoma de Aguascalientes, as the next article we present, *Detection of internal corrosion by long-pulse thermography and digital image processing* by CASTILLO-VALDEZ, Georgina, LARIA-MENCHACA, Julio, GÓMEZ-CARPIZO, Santiago and SANDOVAL-SÁNCHEZ, Juan Antonio, with adscription in the Universidad Politécnica de Altamira, as the last article we present, *Implementation of Matlab communication and Allen Bradley PLC for control of the AMATROL JUPITER XL Robot* by HERNÁNDEZ-JIMÉNEZ, Samuel Abinadí, ORTIZ-VÁZQUEZ, Jonathan, ORTIZ-SIMÓN, José Luis and CRUZ-HERNÁNDEZ, Nicolás, with adscription in the Instituto Tecnológico de Nuevo Laredo.

Content

Article **ECORFAN Journal Democratic Republic of Congo**
June 2023 Vol.9 No.16 1-8

Gunshot detection neural network implemented on a low-cost microcontroller

Red Neuronal para detección de disparos implementada en un microcontrolador de bajo costo

RODRÍGUEZ-PONCE, Rafael†*.

Universidad Politécnica de Guanajuato, Ingeniería en Robótica

ID 1st Author: *Rafael, Rodríguez-Ponce* / **ORC ID**: 0000-0001-5006-5580, **CVU CONAHCYT ID**: 209261

DOI: 10.35429/EJDRC.2023.16.9.1.8 Received March 26, 2023; Accepted June 30, 2023

Abstract

Nowadays, criminal activity is on the rise, and it usually involves some type of firearm. There are automated shot detection systems but in the end, they still require human intervention to decide if it is an actual gunshot. Distinguishing between two similar sounds, such as the detonation of a firearm or a firecracker, is not always possible with the naked ear. There are multiple publications on artificial intelligence to identify gunshots; however, they use convolutional neural networks, which, despite being highly effective, require a system with extensive computational resources. This document presents a fully connected neural network implemented on a microcontroller that can identify up to 90% of firearm detonations. This document will be of interest to students or researchers interested in the design of neural networks for sound recognition on embedded systems.

Artificial Intelligence, Mel frequency cepstral coefficients (MFCC), Micropython, Pytorch, Embedded systems

Resumen

Hoy en día, la actividad criminal se encuentra al alza y usualmente involucra algún tipo de arma de fuego. Existen sistemas de detección de disparos automatizados pero al final, aún requieren de la intervención humana para decidir si en verdad es la detonación de un arma de fuego. Distinguir entre dos sonidos similares, como la detonación de un arma de fuego o un petardo, no es siempre posible a simple oído. Existen múltiples publicaciones en inteligencia artificial para identificar disparos, sin embargo utilizan redes neuronales convolucionales, las cuales, a pesar de tener una alta efectividad, requieren de un sistema con amplios recursos computacionales. Este documento presenta una red neuronal multicapa implementada en un microcontrolador que puede identificar hasta un 90% de detonaciones de arma de fuego. Este documento será de interés a estudiantes o investigadores interesados en el diseño de redes neuronales para reconocimiento de sonidos en sistemas embebidos.

Inteligencia Artificial, Coeficientes cepstrales de frecuencias de Mel (MFCC), Micropython, Pytorch, Sistemas embebidos

Citation: RODRÍGUEZ-PONCE, Rafael. Gunshot detection neural network implemented on a low-cost microcontroller. ECORFAN Journal-Democratic Republic of Congo. 2023, 9-16: 1-8

* Author's Correspondence (e-mail: rrodriguez@upgto.edu.mx)
† Researcher contributing first author.

Introduction

Currently in Mexico, there is a climate of fear and uncertainty, due to the constant acts of violence that occur, day by day, in different parts of the country.

It is common to hear loud noises and immediately attribute them to gunshots, when in fact it can be something as mundane as fireworks, the backfire of a car exhaust, or simply a tire explosion.

To reduce and prevent gun violence in public areas, a growing number of cities in Europe and North America are adopting gunshot detection technology. However, these systems have not been without criticism due to their high maintenance cost, false-positive activation rates and their low efficacy in reducing violence, in addition to the fact that they are not available to the public in general (Aguilar, 2018; Lawrence *et al.*, 2018).

There are multiple publications on gunshot detection projects, nevertheless most are commonly based on the use of convolutional neural networks (Katsis *et al.*, 2022; Morehead *et al.*, 2019) or recurrent neural networks (Olmos *et al.*, 2018). Despite both being highly effective, they require computer systems with extensive processing, memory and graphics card resources, since they analyze the spectrogram image of the detected audio signal (Arif *et al.*, 2021; Bajzik *et al.*, 2020).

In this paper, the author opted for implementing a Fully Connected Neural Network (FCNN) on a low-cost microcontroller with limited computational resources, to have a portable, economical, and low-power gunshot detection system.

To extract the most relevant information from the gunshot audio signal, Mel Frequency Cepstral Coefficients (MFCC) were used since they are the most appropriate digital processing technique for this type of application (Li *et al.*, 2022; Sharma *et al.*, 2019). These coefficients are obtained through a filter bank whose operation is similar to that of the human ear (Jo, Yoo and Park, 2015).

For the recognition of the detonation audio signal, a FCNN was implemented with 10 inputs, two layers, and eight neurons in the hidden layer. Firstly, the audio signal is digitally processed with MFCC and 10 coefficients are obtained. These are fed into the neural network, and at the output there is a single bit indicating on an LED if the sound detected is coming from a firearm or not. The network was trained with more than 3,000 shot sounds from internet databases and detonations recorded at a local shooting range. Similarly, locally generated sounds such as blows, balloon explosions, firecrackers, and car exhaust detonations were used for negative training of the neural network.

This work can be very interesting and useful for students, teachers or researchers interested in the implementation of neural networks to recognize unique sounds on mobile devices.

Artificial Neural Network

An artificial neuron is a computational algorithm inspired by the functioning of biological neurons in the human brain. The neuron, also known as a perceptron, has several data inputs, a processing stage, and a single output. The main benefit of the neuron is that, just like human neurons, it can be trained for various applications, primarily pattern recognition (Aggarwal, 2018).

Each of the neuron inputs has a different weight, which is adjusted during the training process based on the error detected at the output. If a large amount of data is used during training, it is possible to reduce the error in such a way that the neuron can identify a pattern quickly and efficiently.

In order for the algorithm to carry out the learning of more complex processes, multiple neurons are interconnected in multiple layers, thus obtaining a FCNN. In the network, neurons are normally ordered by layers, in such a manner that the outputs of each neuron in one layer are fed to all the neurons in the next layer. Firstly, there is the input layer, where the data to be processed is entered. Next, there can be several hidden layers, and lastly, there is the output layer. The general structure of a FCNN neural network is shown in Figure 1.

ISSN 2414-4924

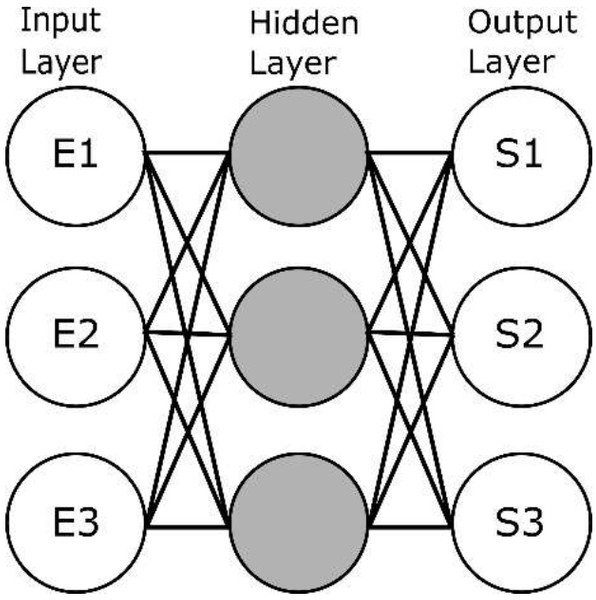

Figure 1 Structure of a fully connected neural network
Source: Self-Made

Currently, there is a great diversity of neural networks for different applications such as event prediction, pattern recognition, image generation, and industrial part design, among many others (Zu and Sutton, 2003).

Gunshot Waveform Analysis

A conventional firearm uses a gunpowder combustion to propel the bullet out of the barrel. Explosive gases expand rapidly, forcing a supersonic jet stream from the muzzle of the weapon. The flash causes an acoustic shock wave and a brief explosive sound that lasts only a few milliseconds. The maximum sound pressure level associated with the flash can exceed 150 dB in the vicinity of the firearm (Maher and Shaw, 2008). If a person is close enough to the gunshot, the sound is unique and unmistakable. Notwithstanding, at a certain distance, surrounded by buildings and mixed with ambient noise, it is not so evident.

In Figure 2 a comparison is made between the sound of a gunshot (a) and the detonation of a car backfire (b). To the naked eye, the waveform of the former does not differ much from the detonation waveform of the latter. Nevertheless, when obtaining the frequency content of both sounds, it is possible to visualize that the spectral content of the gunshot (c) is much broader than that of the exhaust detonation (d).

That is, when for the detonation of the exhaust the frequencies with the highest amplitude ranging from 1000 to 9000 Hz, for the gunshot the frequencies have high amplitude ranging from 3 to 20,000 Hz. This difference becomes even more noticeable once the MFCC coefficients are extracted; it is this difference between signals that is trained into the neural network to be able to recognize the sound of a gunshot.

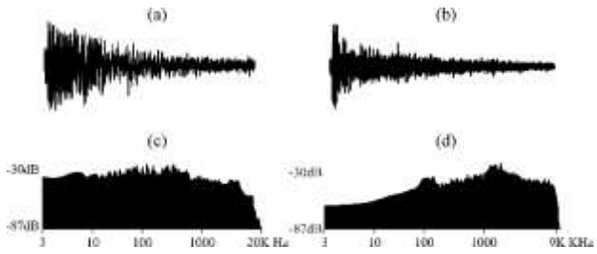

Figure 2 Waveforms for (a) a gunshot and (b) a car backfire detonation. Frequency content of (c) the gunshot and (d) the car backfire detonation
Source: Self-Made.

Audio Signal Information Extraction

A detonation audio signal is composed of numerous frequencies, and therefore cannot be fully processed due to time limitations or computational resources. For this reason, to identify it quickly and effectively, it is necessary to first extract the most relevant information so that it can be properly analyzed (Shi *et al*., 2018).

There are various techniques for extracting information from digital signals, such as the discrete Fourier transform (DFT), the discrete Wavelet transform, linear prediction coefficients, among many others; nonetheless, a technique widely used in detonation detection projects, is by means of the mel frequency cepstral coefficients, or MFCC. This is due to their simplicity and effectiveness, as well as the ease of applying them computationally (Hossan *et al.*, 2010).

To obtain the MFCC, firstly, the DFT transform is applied to extract the spectral content. Next, this information passes through a mel-scale filter bank, which extracts the most relevant data in certain frequency ranges. Finally, the logarithm of these energies is calculated, and the discrete cosine transform is applied to revert them into the time domain.

ISSN 2414-4924

The description of the MFCC process is shown in Figure 3.

With the MFCC technique, it is possible to change the number of coefficients necessary to be obtained from the audio signal, which can usually range between 10 and 25, depending on the application. Selecting more cepstral coefficients only results in a higher complexity in the model. In the case of this project, 10 coefficients were enough to effectively identify the sound of a gunshot.

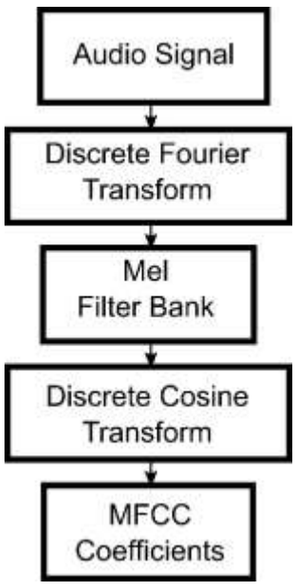

Figure 3 Block diagram for the MFCC information extraction technique
Source: Self-Made

Neural Network Design

Before implementing the gunshot identification system on the microcontroller, it was found beneficial to first design and train the neural network on a personal computer using the Python programming language and PyTorch libraries. This network would only serve as a reference for the design of the network for the microcontroller.

PyTorch is an open-source library based on Python, focused on performing numerical calculations through tensor programming, which facilitates its application in neural network projects. In addition, the simplicity of its interface and its ability to run on graphics processing units (GPUs) make it the most suitable and fastest option for creating artificial neural networks of different sizes and configurations (Chirodea *et al.*, 2021).

Due to the ease with which a neural network can be designed and trained on Pytorch, it was possible to experiment with different sizes and numbers of layers to obtain the smallest and most effective network for the identification of the available audio signals. Thus, it was proven that a neural network of 10 inputs and 2 layers is sufficient for the identification of gunshots with a success rate of up to 100%.

For the neural network training process, a database of more than 3000 gunshot sounds from different types of weapons and calibers was used. The audios were obtained free of charge from the Kaggle website (www.kaggle.com) and from the Gunshot Audio Forensics Dataset website (www.cadreforensics.com/audio/). Both sites contain an extensive database of audio shots of different calibers, including pistols, revolvers, short and long-range rifles (AK-12, AK-47, M16), machine guns, Lugers, and carbines. Similarly, a compendium of 500 shots recorded with a USB microphone at a local shooting range was created. For similar non-firearm audio, sounds such as banging, balloon popping, firecrackers, car backfires, and loud clapping sounds were used.

For the extraction of the most important audio features using MFCC, the Librosa libraries was used, which are a free Python toolkit for audio and music analysis and processing. Some common functions such as time frequency processing, feature extraction and sound graphing are available (McFee *et al.*, 2015). All the sounds to be used were processed with this toolkit, and the corresponding MFCCs were stored in a comma-separated values (CSV) file for use in Pytorch, and also in a text file for use on the microcontroller.

Figure 4 shows the neural network implementation process in Pytorch and is briefly described below.

ISSN 2414-4924

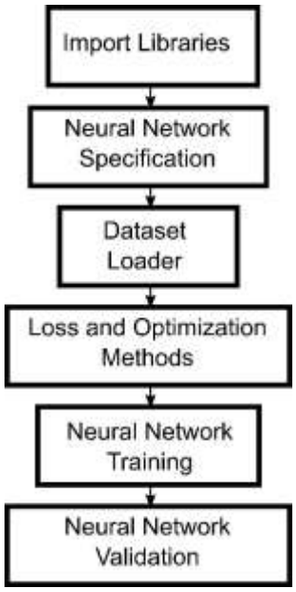

Figure 4 Block diagram for the gunshot identification system on Pytorch
Source: Self-Made.

Firstly, all the libraries required for the project are imported, in this case, the Pytorch libraries for the neural network, Numpy libraries for matrix operations and Pandas libraries for data retrieval from the CSV file. Following, the neurons and the necessary layers for the network are specified, as well as the activation function to be applied on each neuron, which in this project, both the sigmoid function and the hyperbolic tangent function, were tested. Subsequently, the audio MFCCs are retrieved from the CSV file; data and labels are separated and then loaded into the Dataloader.

This loader function is quite useful since it allows loading the data randomly so that the neuron training is not based on the order of the information. Furthermore, the error calculation methods and the optimization of the weights for the neural network are specified; in this case, the binary crossed entropy loss function (BCELoss) and the Stochastic Gradient Descent (SGD) algorithms were used, respectively. Finally, the training of the network is executed. A sample of the Pytorch code where the FCNN class is defined is shown in Figure 5. In this class, two methods must be defined. The first part is the initialization method which is used to create all the necessary layers and activation functions. The second is the forward method where all the layers and activation functions are combined together to create the desired neural network.

```
# Neural network model is defined
class gunshot_fcnn(nn.Module):
    def __init__(self, input_size, hidden_size, output_size):
        super(gunshot_fcnn, self).__init__()
        self.fc1 = nn.Linear(input_size, hidden_size)   # Hidden layer
        self.fc2 = nn.Linear(hidden_size,output_size)   # Output layer
        self.sig = nn.Sigmoid()                         # Activation function

    def forward(self, x):
        out = self.sig(self.fc1(x))                     # Hidden Layer
        out = self.sig(self.fc2(out))                   # Output Layer
        return out
```

Figure 5 Sample of the code in Pytorch for the fully connected neural network definition
Source: Self-Made

For the training of the neural network, 500 epochs with a batch size of 10 audio samples were sufficient. In addition, the verification of the accuracy of the network was carried out using 300 samples that were not included in the training. Table 1 shows the success results obtained with different sizes and configurations of the network with the training data.

Number of Coefficients	Network layers	Activation function	Success rate
5	2	Sigmoid	73.2%
7	2	TanH	82.5%
10	2	Sigmoid	100%
10	2	TanH	100%
15	3	Sigmoid	100%
15	3	TanH	100%

Table 1 List of results obtained in Pytorch using different network sizes and configurations
Source: Self-Made

Gunshot Identification System on the Microcontroller

Once a general idea of the size and configuration required on the neural network was determined in Pytorch, the implementation was carried out on the Espressif Systems ESP-32 microcontroller. Table 2 presents some of the processor main components.

Components	Description
Processor	Dual-core CPU, 32 bits, 240 MHz.
Memory	4 MB SPI Flash, 8MB PSRAM.
Peripherals	ADC, DAC, PWM, Timers, 34 GPIO
Communication	Wi-Fi, Bluetooth, SPI, I2C, UART.

Table 2 List of the ESP32 microcontroller main components
Source: Self-Made

ISSN 2414-4924

For the implementation of the gunshot identification system on the ESP-32, Micropython programming language was used, which despite having the same syntax as Python, cannot use the Librosa libraries for obtaining the MFCC coefficients. Therefore, this extraction algorithm had to be written from the start for the ESP-32. Similarly, Numpy libraries which are used for matrix operations cannot be used on a microcontroller, for this reason, only one audio signal can be processed at a time. Thus, it was expected that the accuracy obtained previously in Pytorch would not be the same on the ESP-32.

In order to expedite the training of the neural network on the microcontroller, the audio files for the 3000 shots and 500 non-shots were previously processed on a personal PC with Librosa to obtain the MFCC coefficients, and then stored in a MicroSD memory card. Subsequently, it was inserted into the ESP-32 development board and the network training was carried out.

To verify the accuracy of the gunshot detection system, the microcontroller first uses a high-sensitivity sound detection module (KY-037). This device includes a condenser microphone to observe changes in environmental noise. When the sensor detects a sound above an adjustable threshold, it provides a high signal to the microcontroller, and an interrupt service routine (ISR) is executed. In this ISR, the microcontroller performs 10-bit analog-to-digital conversions for a duration of 200 ms while appending each sample to a list. Next, the 10 MFCC coefficients are extracted from the list, normalization is applied to the data, and is then fed into the neural network. The network output is displayed on an LED, which stays on for 2 seconds if the audio signal comes from a firearm. Otherwise, it will turn on for only 0.5 seconds. Figure 6 shows the block diagram of the gunshot identification system on the ESP-32.

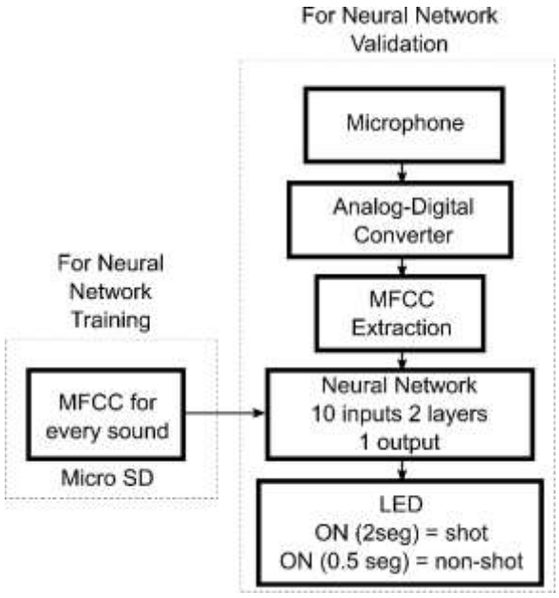

Figure 6 Block diagram for the gunshot detection system executed on the ESP-32 microcontroller
Source: Self-Made

Experimental Results

For the first series of tests of the gunshot detection system on the microcontroller, the sounds were reproduced, one by one, on a personal computer using two 150 W speakers at a volume of approximately 50 dB. The system microphone was placed at a distance of 50 cm from both speakers during the playback of shot and non-shot audios. To verify the success rate, 200 audio recordings of different caliber gunshots and 200 non-gunshots were used. The accuracy rates are shown in Table 3.

A second series of tests was carried out at a local shooting range to test the accuracy of the system with direct detonations of the weapon at different distances. The best results were obtained at a distance of 20 meters from the detonating weapon. When the distance was increased to 100 and 200 meters, the accuracy rate was significantly reduced. These results are attributed to the reduction in the volume of the shot compared to the volume of environmental noise. The results of these tests can also be seen in Table 3.

ISSN 2414-4924

Sounds	Emitted	Asserted	Accuracy
Shots on PC	200	175	87.5 %
Non-shots on PC	200	163	81.5 %
Gunshots at a 20 meters	20	18	90 %
Gunshots at 100 meters	20	13	75 %
Gunshots at 200 meters	20	9	70 %

Table 3 Accuracy rates for the gunshot detection system on the ESP-32 microcontroller
Source: Self-Made

Conclusion

In this work, a fully-connected neural network for the identification of gunshots was presented. This network was implemented on an ESP-32 microcontroller, which is a low-cost and low-power mobile device. With this architecture, up to 90% identification was achieved for firearm sounds and 81.5% for non-firearm sounds.

This work will be of great interest to students, teachers or researchers looking for a simple and efficient alternative for the implementation of fully connected neural networks for sound detection.

References

Aguilar, J.R. (2018). Sistemas de detección de disparos: ¿son eficaces para controlar la violencia con armas de fuego en América Latina?, *URVIO Revista Latinoamericana de Estudios de Seguridad*, *23*(1), 128-141. DOI: 10.17141/urvio.23.2018.3454.

Aggarwal, C.C. (2018). *Neural Networks and Deep Learning: A Textbook*, Ed. Springer. DOI: 10.1007/978-3-319-94463-0.

Arif, E., Shahzad, S.K., Mustafa, R., Jaffar, M.A. and Iqbal, M.W. (2021). Deep Neural Networks for Gun Detection in Public Surveillance, *Intelligent Automation and Soft Computing*, *32*(2), 909-922. DOI: 10.32604/iasc.2022.021061.

Bajzik, J., Prinosil, J. and Koniar, D. (2020). *Gunshot Detection using Convolutional Neural Networks*, 24th International Conference Electronics, Palanga, Lithuania. DOI: 10.1109/IEEECONF49502.2020.9141621

Jo, J., Yoo, H. and Park, I.C. (2015). Energy-Efficient Floating-Point MFCC Extraction Architecture for Speech Recognition Systems, *IEEE Trans. VLSI Syst*., *24*(2), 754-758. DOI: 10.1109/TVLSI.2015.2413454.

Katsis, L.K.D., Hill, A.P., Piña-Covarrubias, E., Prince, P., Rogers, A., Doncaster, C.P. and Snaddon, J.L. (2022). Automated detection of gunshots in tropical forests using convolutional neural networks, *Ecological Indicators*, *141*(1), 1-9. DOI: 10.1016/j.ecolind.2022.109128.

Lawrence, D.S., La Vigne, N.G., Goff, M. and Thompson, P.S. (2018). Lessons Learned Implementing Gunshot Detection Technology: Results of a Process Evaluation in Three Major Cities, *Justice Evaluation Journal*, *1*(2), 109-129. DOI: 10.1080/24751979.2018.1548254.

Li, J., Guo, J., Ma, M., Zeng, Y., Li, C. and Xu, J. (2022). A Gunshot Recognition Method Based on Multi-Scale Spectrum Shift Module, *Electronics*, *11*(1), 1-12. DOI: 10.3390/electronics11233859

Morehead, A., Ogden, L., Magee, G., Hosler, R., White, B. and Mohler, G. (2019). *Low Cost Gunshot Detection using Deep Learning on the Raspberry Pi*, IEEE International Conference on Big Data (Big Data), Los Angeles, California. DOI: 10.1109/BigData47090.2019.9006456.

Olmos, R., Tabik, S. and Herrera, F. (2018). Automatic handgun detection alarm in videos using deep learning, *Neuro Computing*, *275*, 66–72. DOI: 10.1016/j.neucom.2017.05.012.

Sharma, G., Umapathy, K. and Krishnan, S. (2019). Trends in audio signal feature extraction methods, *Applied Acoustics*, *158*(1), 1-19. DOI: 10.1016/j.apacoust.2019.107020.

Zu, J. and Sutton, P. (2003). *FPGA Implementations of Neural Networks - A Survey of a Decade of Progress*, Ed. Springer-Verlag, Berlin, 1062-1066. DOI: 10.1007/978-3-540-45234-8_120.

ISSN 2414-4924

Maher, R.C. and Shaw, S.R. (2008). *Deciphering Gunshot Recordings*, AES 33rd International Conference, Denver, Colorado, 1-8. https://www.researchgate.net/publication/228900815_Deciphering_Gunshot_Recordings.

Shi, L., Ahmad, I., He, Y. and Chang, K. (2018). Hidden Markov model based drone sound recognition using MFCC technique in practical noisy environments, *Journal of Communications and Networks*, 20(5), 509-518. DOI: 10.1109/JCN.2018.000075.

Hossan, M.A., Memon, S. and Gregory, A. (2010). *A novel approach for MFCC feature extraction*, 4th International Conference on Signal Processing and Communication Systems, Gold Coast Australia. DOI: 10.1109/ICSPCS.2010.5709752.

Chirodea, M.C., Novac, O.C., Novac, C.M., Bizon, N., Oproescu, M. and Gordan, C.E. (2021). *Comparison of Tensorflow and PyTorch in Convolutional Neural Networks - based Applications*, 13th. Int. Conf. on Electronics, Computers and Artificial Intelligence, Pitesti, Romania. DOI: 10.1109/ECAI52376.2021.9515098.

McFee, B., Raffel, C., Liang, D., Ellis, DPW., McVicar, M., Battenberg, E. and Nieto, O. (2015). *Librosa: audio and music analysis in Python*, In Proceedings of the 14th Python in science conference, 18-25. DOI: 10.5281/zenodo.6097378.

ISSN 2414-4924

Article **ECORFAN Journal-Democratic Republic of Congo**
June 2023 Vol.9 No.16 9-21

Transfer Learning to improve the Diagnosis of Type 2 Diabetes Mellitus (T2D)

Transfer Learning para mejorar el Diagnostico de Diabetes Mellitus Tipo 2 (T2D)

CUTIÉ-TORRES, Carmen†*, LUNA-ROSAS, Francisco Javier, LUNA-MEDINA, Marisol and DUNAY-ACEVEDO, Cesar

TecNM/Instituto Tecnológico de Aguascalientes, Departamento de Sistemas y Computación, Av. A. López Mateos 1801 Ote. Fracc. Bona Gens, Aguascalientes, Aguascalientes, México. C.P. 202564
Universidad Autónoma de Aguascalientes, Centro de Ciencias de la Salud, Av. Universidad # 940 Col. Universitaria C.P. 20131, Aguascalientes Ags., México

ID 1st Author: *Carmen, Cutié-Torres* / **ORC ID:** 0009-0000-9210-5667, **CVU CONAHCYT ID**: 1156355

ID 1st Co-author: *Francisco Javier, Luna-Rosa* / **ORC ID:** 0000-0001-6821-4046, **CVU CONAHCYT ID:** 87098

ID 2nd Co-author: *Marisol, Luna-Medina* / **ORC ID:** 0009-0006-0188-9317, **CVU CONAHCYT ID:** 1303944

ID 3rd Co-author: *Cesar, Dunay-Acevedo* / **ORC ID:** 0009-0001-9370-2997, **CVU CONAHCYT ID:** 1303869

DOI: 10.35429/EJDRC.2023.16.9.9.21 Received March 28, 2023; Accepted June 30, 2023

Abstract

Transfer Learning is a Deep Learning technique that is currently being used in early and non-invasive diagnosis of T2D. The objective of this work is to design and implement a Transfer Learning model trained with images of skin patches belonging to healthy people and diabetic foot patients. The research methodology was constituted by 3 phases (Analysis and Design, Development and Evaluation) composed of 5 steps that comply with the proposed objective. Several convolutional neural network (CNN) models were developed: CNN built from scratch, AlexNet, CNN with data augmentation technique, FE-VGG16, FE-ResNet50 and FT-VGG16. These models were evaluated using a set of metrics derived from the confusion matrix, the Receiver Operating Characteristic curve (ROC) of each model and the value corresponding to the area under the curve (AUC). The best performance corresponded to FT-VGG16 model that fuses VGG-16 pretrained model with a block of fully connected layers. Finally, satisfactory results are reported and allow us to conclude that the application of Transfer Learning models for the classification of diabetic foot images constitutes a viable tool for the non-invasive diagnosis of T2D.

Transfer Learning, Classification, Diagnosis

Resumen

Transfer Learning es una técnica de Aprendizaje Profundo que está siendo utilizada actualmente en el diagnóstico temprano y no invasivo de T2D. El objetivo de este trabajo es diseñar e implementar un modelo de Transfer Learning entrenado con imágenes de parches de piel pertenecientes a personas sanas y enfermos de pie diabético. La metodología de la investigación se constituyó por 3 fases (Análisis y Diseño, Desarrollo y Evaluación) compuestas por 5 pasos que dan cumplimiento al objetivo propuesto. Se desarrollaron 6 modelos de redes neuronales convolucionales (CNN): CNN construida desde cero, AlexNet, CNN con técnica de aumento de datos, FE-VGG16, FE-ResNet50 y FT-VGG16. Estos modelos fueron evaluados mediante un conjunto de métricas derivadas de la matriz de confusión, la curva ROC (característica operativa del receptor) de cada modelo y el valor correspondiente al área bajo la curva (AUC). El mejor desempeño correspondió al modelo FT-VGG16 que fusiona el modelo preentrenado VGG-16 con un bloque de capas completamente conectadas. Finalmente, se reportan resultados satisfactorios que permiten concluir que la aplicación de modelos de Transfer Learning para la clasificación de imágenes de pie diabético constituye una herramienta viable para el diagnóstico no invasivo de T2D.

Transferencia de Aprendizaje, Clasificación, Diagnóstico

Citation: CUTIÉ-TORRES, Carmen, LUNA-ROSAS, Francisco Javier, LUNA-MEDINA, Marisol and DUNAY-ACEVEDO, Cesar. Transfer Learning to improve the Diagnosis of Type 2 Diabetes Mellitus (T2D). Journal-Democratic Republic of Congo. 2023, 9-16: 9-21

* Correspondence to Author (e-mail: ccutietorres@gmail.com)
† Researcher contributing first author.

1. Introduction

Diabetes mellitus is currently a chronic disease with high incidence rates worldwide. There are several types of diabetes, including type 2 diabetes (T2D) which is closely related to the body's response or resistance to the hormone insulin and endocrine pancreatic beta cell dysfunction (WHO Library Cataloging-in-Publication Data, n.d.).

T2D has a prevalence of 10.3% in Mexico according to the 2021 National Health and Nutrition Survey (ESNAUT), which indicated that more than 12 million people over the age of 20 live with this disease. The country's death rate was 11.0 per 10,000 inhabitants, of which 74.9% corresponded to T2D and only 48% were affiliated with a Health Institution (INEGI, 2022).

Several complications associated with T2D include cardiovascular diseases, neuropathy, nephropathy, diabetic retinopathy, ulcerations and frequent infections.

Diabetic foot ulcer has become a condition that affects the quality of life of patients with T2D due to the high numbers of amputations and mortality that it entails. According to the reports of the Hospital Type 2 Diabetes Mellitus Epidemiological Surveillance System for 2022, the diabetic foot is recognized as one of the most frequent causes of admission (12.5% of total admissions), which includes patients who did not know they were sick previously (Salud, n.d.).

The American Diabetes Association (ADA) recognizes glycosylated hemoglobin (A1C), fasting plasma glucose (FPG), the Oral Glucose Tolerance Test (OGTT) and the Random plasma glucose test as clinical methods for manual diagnosis of diabetes. These are tests performed by venous puncture, in health centers or outpatient units with the presence of personnel specialized in the manipulation of blood fluids (American Diabetes Association, n.d.).

Other devices for daily use are the traditional glucometer or the Continuous Glucose Monitoring (CGM) systems. These methods require venous or intramuscular puncture, causing frequent discomfort and infections to the patient (Patel & Priefer, 2021).

Nevertheless, despite its existence, between 30% and 80% of D2T cases are not detected promptly due to the slow progression of the disease symptoms (OMS, n.d.).

Scientific community has adopted different approaches to improve the detection and early diagnosis of T2D, including non-invasive methods, the use of advanced technologies, awareness, and education about the disease. These efforts are aimed at reducing the lethal consequences of T2D and improving the quality of life for those affected.

In this regard, they highlight the use of Artificial Intelligence (AI) algorithms in tasks of classifying medical images or data from patient medical records. Numerous models based on Machine Learning and Deep Learning techniques make it possible to diagnose T2D with precision, sensitivity, and specificity criteria like those perceived by medical specialists. They also allow large data sets to be analyzed quickly and accurately, which can help identify disease-related patterns and correlations (Afsaneh *et al*., 2022; Fregoso-Aparicio *et al*., 2021; Silva *et al*., 2021).

The goal of this research is to develop a computational model based on Transfer Learning techniques for non-invasive diagnosis of T2D using images of diabetic feet from both healthy and diseased patients.

The proposed approach seeks to provide an effective and reliable solution in the early detection of T2D, which could allow timely treatment and improve the quality of life of patients.

Our paper is structured as follows: in Section 2 concepts of interest are introduced, as well as a brief state of the art related to the non-invasive diagnosis of T2D. Section 3 presents the methodology used which is divided into 3 phases with 5 fundamental steps or activities. In Section 4 we discuss the results, while in Section 5 we acknowledge the contributions received. In Section 6 we determine the conclusions and contributions of our work. In Section 7 we show the references bibliography used through the investigation.

ISSN 2414-4924

2. Related Works

Machine Learning (ML) is a subset or discipline of the AI field made up of algorithms that learn automatically and identify patterns in the data. This data is supplied to them during their training stage. Notwithstanding, ML algorithms do not need to be programmed with specific rules and can be applied to both classification and regression tasks. They are divided into 3 categories: Supervised Learning, Unsupervised Learning, and Reinforcement Learning.

Deep Learning (DL) is considered a subset of ML, since they are nourished by the basic principles of Artificial Neural Networks (ANN) inspired by the interconnection and functioning of neurons in the human brain. Like these, deep learning networks are composed of layers of neurons that learn progressively, using algorithms such as backpropagation during the training process. The difference between ANNs and DL consists in the depth or number of stacked layers (more than three layers) that make up a DL model, which provide greater complexity and the ability to discover patterns in large data collections.

To carry out the non-invasive diagnosis of T2D using Machine Learning, Carter *et al*. (2019) used Random Forests to classify diabetic nails, Zhang *et al*. (2021) developed models with Boosting and Bagging techniques to deal with unbalanced data from diabetic patients, Agrawal *et al*. (2022) applied Logistic Regression algorithms, k nearest neighbors, Decision Trees, Support Vector Machines in D2T classification tasks with a dataset obtained using the iGLU 2.0 serum glucometer (Jain *et al*., 2020). Also, Sanchez-Brito *et al*. (2022) use Artificial Neural Networks to classify the disease using patient saliva spectra obtained using Attenuated Total Reflectance -Fourier Transform InfraRed (ATR-FTIR) spectroscopy technique.

Within Deep Learning, publications highlight the growing interest in the use of Convolutional Neural Networks (CNN) given its ability to detect patterns in medical images. The high sensitivity of these models, as well as their specificity when discriminating between different classes, makes them potential diagnostic tools.

Qiao *et al*. (2020) classified different stages of diabetic retinopathy (early, moderate, and severe non-proliferative diabetic retinopathy) using fundus images. Semantic segmentation algorithm capable of distinguishing between an infected and normal retina was implemented to detect early signs such as microaneurysms or macular edema.

Tang *et al*. (2020) developed a CNN-based framework and fuzzy-c means algorithm models to predict the onset of type 2 diabetes one year in advance using quantitative patient information and abdominal computed tomography images.

Cruz-Vega *et al*. (2020) implemented AlexNet and GoogleNet pretrained models based on Transfer Learning and in turn proposed a new structure trained from scratch with plantar thermography images of diabetic patients.

Munadi *et al*. (2022) also delved into the use of thermal imaging and reported a model based on MobileNetV2 and ShuffleNet. The binary classification resulting from both models was merged or combined using the Fusion Decision technique (Wang *et al*., 2017).

Solutions such as DFUNet (Goyal *et al*., 2020), DFU_QUTNet (Alzubaidi *et al*., 2020), YOLOv5, Faster R–CNN, EfficientDet (Yap *et al*., 2021) and CKB-DeiT-B-D (Xu *et al*., 2022) also made contributions in the classification of images of diseased epidermal tissue or ulcerations.

3. Methodology

We propose a methodology consisting of 3 fundamental Phases: Analysis and Design, Development and Evaluation. These phases contemplate a group of steps or activities that allow the objective of the investigation to be fulfilled:

– Analysis and Design Phases: Firstly, a search and acquisition of the dataset that best fits our object of study is carried out. Afterwards, the different Deep Learning models that will intervene in the training and validation stages are designed.

ISSN 2414-4924

– Development Phase: The steps of this phase include the execution of the training of each model designed in the previous stage.

– Evaluation Phase: Finally, the models are validated through a group of performance metrics equivalent to those used in clinical trials.

3.1 Dataset acquisition

The Diabetic Foot Ulcer (DFU) dataset used in this research was obtained from the Kaggle.com website (*Diabetic Foot Ulcer (DFU)*, n.d.). According to the authors Alzubaidi *et al*. (2022) the dataset was generated at the Al-Nasiriyah Center for Endocrinology and Diabetics in Iraq and is composed of patches of damaged or healthy skin. These patches were obtained by detecting and segmenting Regions of Interest (ROI) that were labeled by medical experts according to their respective classes.

The dataset contains a total of 1055 images with dimensions of 224 x 224, which were classified into Abnormal (ulcerated skin) and Normal (healthy skin), with 512 and 543 files respectively.

3.2 Model Design

Brief Explanation of Convolutional Neural Networks (CNN)

The CNN is a type of deep neural network made up of several hidden layers used in the field of machine vision and object recognition due to its ability to try to mimic the human visual cortex.

As same as Artificial Neural Networks, it uses the backpropagation algorithm in its learning, with a hierarchical structure that allows its layers to extract patterns in the data from low (lines, curves, contours, etc.) to high level (complex shapes, objects, faces, etc.), based on the order in which they are stacked.

The main elements of CNNs are:

– Convolution layers: Hidden layers in which multiplicative operations are executed between the matrix made up of the RGB channels of the input image in a range of 0 to 255 pixels, and the kernel, also known as a filter, convolution matrix, or synaptic weight matrix. These are responsible for activating different characteristics of the image. As Figure 1 indicates, the convolution is performed iteratively calculating the dot product between portions of the input matrix and the kernel. This operation moves until all the elements of the feature map, also known as 3D tensor, are covered.

Mathematically it can be stated with the following equation:

$$f \circledast h = g \quad (1),$$

where f and h correspond to different functions, and g is the output or feature map.

In a convolutional layer, the kernel and the bias are considered trainable parameters that are optimized by algorithms based on gradient descent. This technique uses the calculation of the partial derivative of the loss function with respect to the different parameters mentioned above.

– Pooling Layers: They are used to reduce the dimension of the matrices resulting from the convolution by subsampling the input, which allows preserving its most representative characteristics. There are several ways to condense these matrices, for example: Max-pooling that calculates the maximum value of a portion of the total elements, and Average-Pooling that calculates the mean. The stride parameter specifies the step or jump of the displacement of the pooling window in the array.

– Flatten Layers: Converts the 3D tensor to a 1D or vector to serve as input to a group of fully connected layers.

ISSN 2414-4924

– Activation function: It is located at the output of each neuron and constitutes the threshold or limiting function that modifies its result, in such a way that it can continue with the propagation of its value towards another neuron. There are several types: step, sigmoidal, rectifying (ReLU), hyperbolic tangent, softmax, among others.

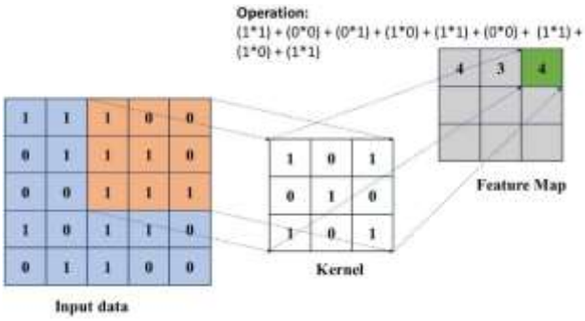

Figure 1. Convolution operation.
Source: Own Elaboration

Simple CNN

The architecture of the simple or built from scratch CNN model consisted of 2 convolutional (2D) layers followed by a MaxPooling layer to reduce the dimensions of the extracted feature maps. In each case the activation function was ReLU. The features that were obtained from the convolution step were flattened using a Flatten layer.

Classification task was performed using two fully connected layer and an output layer, with 50 and 1 neuron respectively. The activation functions were ReLU and sigmoid for classification, as shown in Table 1.

Layer	Kernel size / Filter	Activation function
Conv2D	3 x 3 x 32	ReLU
MaxPool2D		
Conv2D	3 x 3 x 64	ReLU
MaxPool2D	-	-
Flatten	-	-
Dense	50	ReLU
Dense	50	ReLU
Dense	1	sigmoid

Table 1. Simple CNN Architecture
Source: Own Elaboration

Based on AlexNet

In this section we present a model based on the AlexNet network architecture, developed by Krizhevsky *et al*. (2012). AlexNet includes more complex elements compared to the simple CNN, such as Dropout regularization layers used to reduce overfitting of the data by turning off neurons with little significance to the model.

The original model is composed of 5 convolutional layers (Conv2D) with ReLU type activation functions. The first, second and fifth layers followed by 3 pooling layers that seek to condense the information from the previous layer or reduce its dimensionality.

Our proposed model adds Batch Normalization layers after each reduction layer, since it allows to reduce internal covariate changes between minibatches (Ioffe & Szegedy, 2015).

The first layer is composed of filters with dimensions of 11x11, the second with 5x5, and 3x3 in the rest of the convolution layers. Details related to this architecture are shown in Table 2.

We used the Python library called OpenCV to adapt the dataset to the dimensions required by the neural network. In this way, all the images in the dataset were resized to have a size of 227x227 pixels, allowing them to be compatible with the input of the neural network.

Layer	Kernel size / Filter	Activation function
Conv2D	11 x11 x 96	ReLU
BatchNormalization	-	-
MaxPool2D	-	-
Conv2D	5 x 5 x 256	ReLU
BatchNormalization	-	-
MaxPool2D	-	-
Conv2D	3 x 3 x 384	ReLU
BatchNormalization	-	-
Conv2D	3 x 3 x 384	ReLU
BatchNormalization	-	-
Conv2D	3 x 3 x 256	ReLU
BatchNormalization	-	-
MaxPool2D	-	-
Flatten	-	-
Dense	4096	ReLU
Dropout (0.5)		
Dense	4096	ReLU
Dropout (0.5)	-	-
Dense	1	Sigmoid

Table 2. AlexNet Architecture
Source: Own Elaboration

ISSN 2414-4924

Data Augmentation

One of the fundamental problems when analyzing medical images with Deep Learning is the lack of high-quality labeled data. In the medical field, the acquisition of medical data, such as magnetic resonance imaging (MRI), computed tomography (CT), or x-rays, often involves significant costs and resources.

Medical images are often highly varied and contain detailed and complex information. This makes the task of training Deep Learning models even more difficult, as a large amount of diversified and representative data would be needed to capture the variability of medical images and ensure that the model can generalize correctly.

Data augmentation is a technique used to increase the amount and diversity of training data available. It consists of applying random transformations to the existing data to create new samples, which helps improve the performance and generalization of the model to new instances.

In this context, it is useful since we have a limited set of images for a classification problem (1055 elements), which can lead to overfitting problems.

For these purposes, we implemented the ImageDatagenerator class through Keras library, in charge of generating batches of images indefinitely, as shown in Figure 2.

The transformations applied to our dataset of diabetic foot images are detailed below:

- Rotation_range: Rotation of images with respect to the angle denoted in degrees (0-360 degrees).
- Width_shift_range: Random horizontal shift.
- height_shift_range: Random vertical shift.
- Shear_range: Cropping of the image along an axis creating new angles of perception.
- Zoom_range: Increase on the image both horizontally and vertically.
- Horizontal_flip: Flip the image horizontally.
- Fill_mode: Filling of empty pixels with the value of the closest pixels.

Finally, we applied this technique to the training dataset and developed the model using the Simple CNN model architecture described in previous sections.

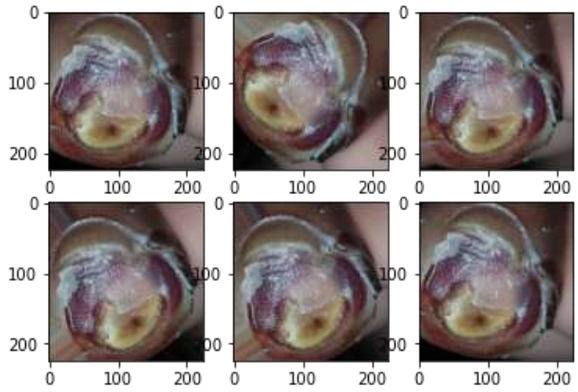

Figure 2 Rotation of an image at an angle of 45 degrees.
Source: Own Elaboration

Transfer Learning

Transfer learning is a technique that allows taking advantage of the knowledge acquired by a model trained in a broad task to be used in a more specific one with a more limited data set. In the present investigation, pretrained models were used in the Imagenet database since it contains more than 14 million annotated images and is designed to be used in visual recognition tasks.

The advantage of this approach is that the pretrained models have already learned to extract relevant features from the images, such as edges, textures, or objects. Taking advantage of this knowledge and adjusting it to the specific task of medical image classification provides higher performance with less data. Therefore, computational costs are reduced by accelerating the training stage of the model since it has optimized weights, thereby reducing the number of parameters to train.

We propose an architecture with a separation of tasks into two blocks as shown in Figure 3. This allows a modular approach in model training. The first part, which includes the convolution and pooling layers, is kept fixed or "frozen", which means that its weight matrices are not updated during training.

ISSN 2414-4924

On the other hand, the second block that contains the fully connected layers is trained with the data from the diabetic foot image dataset. It is here where the essential modifications of the network occur by updating its most important parameters. This step allows the model to specialize in the task of classifying the two classes of foot patches: abnormal and normal.

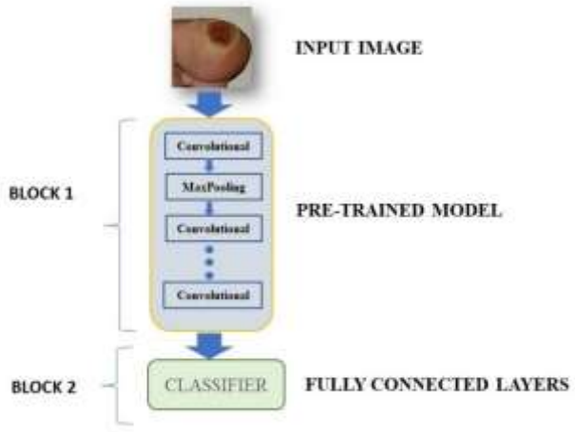

Figure 3. Transfer Learning Approach
Source: Own Elaboration

Feature Extraction

In this section, the VGG16 and ResNet50 pretrained models were developed for the extraction of relevant features according to the modular approach of Transfer Learning discussed in the previous section.

According to the scientific literature (Hacisoftaoglu *et al*., 2020; Hossain *et al*., 2022; Jiang *et al*., 2021; Kathamuthu *et al*., 2023; Shukla & Tiwari, 2022) these models achieve good results in the classification of medical images, are easy to implement and consume fewer physical resources compared to other deeper networks.

The VGG-16 architecture consists of 2 blocks of 2 2D convolutional layers and 3 blocks of 3 2D convolutional layers with filters of size 3 X 3. Each block is followed by a MaxPooling2D layer.

Similarly, the ResNet50 model, which is a variant of the 50-layer CNN, incorporates the use of residual connections which help mitigate the Vanishing gradient problem. Its architecture is defined by identity blocks and convolutional blocks with 1x1, 3x3 and 1x1 filters.

In both cases, the classification task is performed by a set of fully connected layers with two Dense layers of 50 neurons with ReLU activation function and an output layer with a single neuron with sigmoid activation function.

Fine Tuning

A transfer learning technique called fine tuning is used to modify a pretrained model by training some or all its layers with more task-specific data. For this case, we used the architecture used in the previous feature extraction model with VGG-16.

We divided the training into two fundamental stages: freezing the first layers of the model considered low-level due to their ability to extract generic features, and retraining the higher-level layers that are responsible for extracting more specific patterns. In this second stage, the weights of the unfreezed layers do change.

To obtain the proposed model, convolution block number 5 (block5_conv1) was unfrozen within the VGG-16 pretrained model. This block allows training a total of 7,079,424 parameters.

3.3 Model Training

The implementation of the solutions was carried out using the Keras and TensorFlow frameworks. We used Anaconda development environment with Python programming language.

The models were trained for 50 epochs with 75% of the data set. For validation, 15% of the total was used and the remaining 10% was reserved for the prediction of new entries. The optimizer used in all cases was RMSProp with a learning rate of 0.000001. Considering that we are dealing with a two-class classification problem: sick and healthy, we selected binary_crossentropy loss function.

Also, Mini-Batch Gradient Descent was selected as the learning algorithm. Therefore, the Batch Size of the model is equivalent to 20 batches, which indicates the number of samples that will be analyzed before updating the error value, the weight and bias matrix.

ISSN 2414-4924

This technique helps to optimize internal memory consumption when working with limited computational resources. It also allows parallelizing the gradient computation by splitting mini batches across multiple cores or processing devices, which can be especially useful on systems with multiple processing units, such as GPUs.

3.4 Model Validation

To evaluate the ability of the models to correctly classify diabetic and healthy patients, a set of metrics based on the Confusion Matrix were calculated as shown in Table 3. The ROC curve is also used to demonstrate the performance of each model for testing data set.

The 4 cells of the Matrix refer to: True Positives (TP), False Positives (FP), True Negatives (TN), and False Negatives (FN) cases.

		Prediction	
		Positive	Negative
Real	Positive	TP	FN
	Negative	FP	TN

Table 3. Classification results in positive and negative classes.
Source: Vanacore et al. (2022)

Formulas for calculating each metric are defined below:

Accuracy:

$$Acc = (TN + TP)/(TN + FP + FN + TP) \quad (2)$$

Positive Precision o Sensitivity (PP):

$$PP = (TP)/(FN + TP) \quad (3)$$

Negative Precision o Specificity (PN):

$$NP = (TN)/(FP + TN) \quad (4)$$

False positives (PFP):

$$PFP = (FP)/(FP + TN) \quad (5)$$

False negatives (PFN):

$$PFN = (FN)/(FN + TP) \quad (6)$$

Positive Assertiveness (PA):

$$PA = (TP)/(FP + TP) \quad (7)$$

Negative Assertiveness (NA):

$$NA = (TN)/(FN + TN) \quad (8)$$

3.5 Comparative analysis of models

In this last step of the methodology, the results obtained for the 6 Deep Learning models that were coded are compared. We implemented a number of 7 metrics derived from the Confusion Matrix, the loss function value, and the AUC value. The graphs of the loss function and the ROC curve were also analyzed. The results are shown in Table 4 and Table 5. They are discussed in the next section.

4. Results and discussion

In this work, 6 CNN models were developed for the classification of type 2 diabetes by analyzing images of the diabetic foot. To this end, the Keras and Tensorflow development frameworks were used.

Models were trained and tested over 50 epochs, and data augmentation techniques were employed during training to avoid overfitting and improve exposure to diverse features. To partition the dataset and evaluate the performance of the models, we used the train-test Split technique with 75% of the data for training, 15% for validation, and 10% reserved for predictions. The results obtained are shown in Table 4 and 5.

All models used the Data Augmentation technique applied only to train dataset, but Simple CNN model, which was exposed to 797 images of healthy and diseased feet during its training and to 200 images during validation.

Model	Acc	Loss	PP	NP	PFP
Simple CNN	95.49	0.035	100	92.71	7.29
AlexNet	96.49	0.045	95.19	95.83	4.17
DA	97	0.03	96.15	97.92	2.08
FE-VGG16	99	0.01	100	97.92	2.08
FE-ResNet50	98	0.02	100	95.83	4.17
FT-VGG16	99.50	0.005	100	98.96	1.04

Table 4 Performance metrics results for each model (Part 1)
Source: Own Elaboration

ISSN 2414-4924

Model	PFN	PA	NA
Simple CNN	0	93.69	100
AlexNet	4.81	96.12	94.85
DA	3.85	98.04	95.92
FE-VGG16	0	98.11	100
FE-ResNet50	0	96.30	100
FT-VGG16	0	99.05	100

Table 5 Performance metrics results for each model (Part 2)
Source: Own elaboration

As we saw in reported values, all models exhibit results above 95%. Similarly, Graphic 1 shows Accuracy values plotted in function of the training epochs. The FE-VGG16, FT-VGG16 and AlexNet models achieved the best results in their training phase.

Since first epochs the Accuracy values are above 85%, which indicates that models capture a greater number of characteristics in early periods of training. On the other hand, no signs of overfitting were observed for these models since their trend is upward in the case of Accuracy. When analyzing the behavior of the loss function showed in Graphic 2, a downward tendency can be seen in its values, which are in ranges of less than 4%.

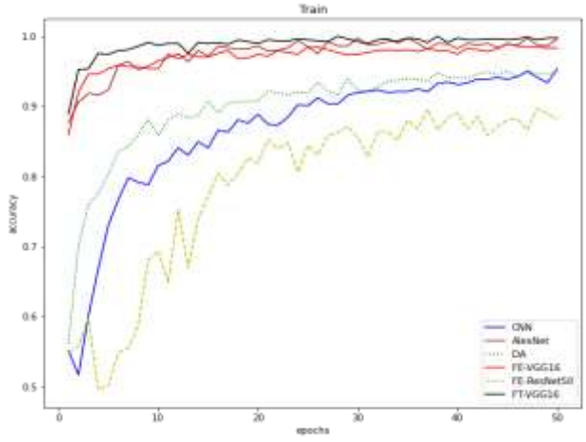

Graphic 1. Accuracy graphs of the models. CCN: Simple Convolutional Neural Network, DA: Data augmentation, FE-VGG16: Feature extraction with VGG-16 pretrained model, FE-ResNet50: Feature extraction with ResNet50 pretrained model, FT: Fine tuning with VGG-16 pretrained model
Source: Own Elaboration

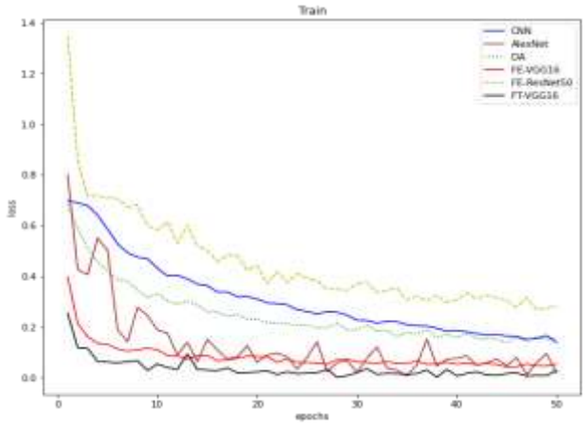

Graphic 2. Loss graphs of the models. CCN: Simple Convolutional Neural Network, DA: Data augmentation, FE-VGG16: Feature extraction with VGG-16 pretrained model, FE-ResNet50: Feature extraction with ResNet50 pretrained model, FT: Fine tuning with VGG-16 pretrained model.
Source: Own Elaboration

Graphic 3 shows the ROC curve of all models. This graph is important to analyze the behavior of the Sensitivity and Specificity values of the models, as well as their diagnostic capacity. It is used in clinical trials since it allows evaluating the ability of the proposed methods to correctly differentiate classes (Martínez Pérez & Pérez Martin, 2023). The results of the metric called AUC, which shows in numerical values the benefits of each model compared to the non-discrimination line with a value of 0.50, were also analyzed.

Accuracy, Sensitivity, Specificity values and others reported in Table 4, made possible to conclude that the best performances are obtained by models that implement Transfer Learning techniques such as feature extraction and fine tuning. In this regard, those that use the pretrained model VGG-16 stand out over the rest.

AlexNet model also reports good results even though its Accuracy value is similar to model with Data Augmentation techniques. Nertheless, AUC value is 100% in the first case. We assumed that this is due to the depth of the model evidenced in the number of hidden layers and activation neurons.

Also, to the use of regularization layers such as Batch Normalization and Dropout that help to avoid overtraining the model.

ISSN 2414-4924

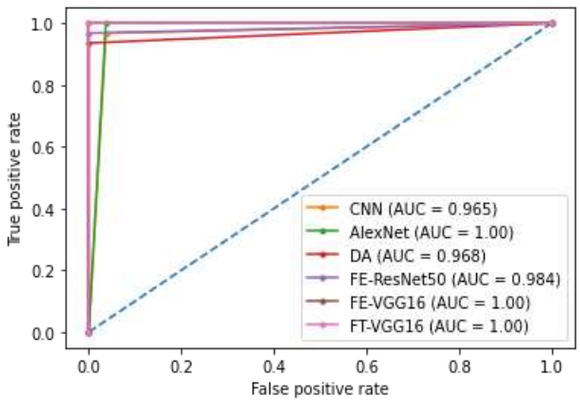

Graphic 3 Area under the curve per models
Source: Own Elaboration

Finally, Figure 6 shows the predictions obtained using the FT-VGG16 model. The prediction process occurs by exposing the trained model to new data to check if it has really learned to detect relevant patterns in the images. In this case, a total of 58 images are processed (27 corresponding diseased skin patches and 31 healthy ones) that were not used in the previous training and validation phases. All were correctly classified, which validates the results of the metrics mentioned above.

5. Acknowledgement

We thank the Technological Institute of Aguascalientes (ITA) and the National Council of Science and Technology (CONAHCYT) for their support in this research.

6. Conclusions

At present day, a continuous rise is projected in the cases diagnosed with T2D. In proportion to these statistics, an increase in the health complications is expected.

The early diagnosis of this disease and the incorporation of healthier lifestyles in people constitute key elements to avoid the high prevalence rates of this deadly condition.

Figure 6 Generation of new predictions for the two classes of skin patches (Model FT-VGG16).
Source: Own Elaboration

Improving the quality of life of patients is also an objective for the scientific community. Less invasive diagnostic variants have been explored that contribute to saving costs. They are efficient and guarantee timely diagnosis using Information Technology (IT) and electronic devices related to the Internet of Things (IoT) paradigm.

Consequently, the present work implements a group of Deep Learning models to classify T2D using diabetic foot images. It is important to consider that in Mexico diabetic foot is one of the most frequent causes of admission in patients without a previous diagnosis.

As a final solution, the FT-VGG16 model is proposed, which merges data augmentation and Transfer Learning techniques. They include the use of the VGG-16 pretrained model for the extraction of relevant features from the set of input images and the fine adjustment with the purpose of further specialize the final layers of the pretrained model, since they are the ones that detect the highest level features in the network. The proposed model presented a very favorable performance, standing out for a global precision of 99.5%, sensitivity of 100%, specificity of 98.96% and AUC of 100%.

ISSN 2414-4924

With this research we hope to contribute to the knowledge generation in medical image classification´s field, especially those related to T2D. Performance evaluation of models based on metrics consistent with the work carried out by health professionals provides a theoretical and practical framework. It validates the application of Transfer Learning techniques within the decision making and disease diagnosis process.

7. References

Afsaneh, E., Sharifdini, A., Ghazzaghi, H., & Ghobadi, M. Z. (2022). Recent applications of machine learning and deep learning models in the prediction, diagnosis, and management of diabetes: A comprehensive review. *Diabetology & Metabolic Syndrome*, *14*(1), 196. https://doi.org/10.1186/s13098-022-00969-9

Agrawal, H., Jain, P., & Joshi, A. M. (2022). Machine learning models for non-invasive glucose measurement: Towards diabetes management in smart healthcare. *Health and Technology*, *12*(5), 955–970. https://doi.org/10.1007/s12553-022-00690-7

Alzubaidi, L., Fadhel, M. A., Al-Shamma, O., Zhang, J., Santamaría, J., & Duan, Y. (2022). Robust application of new deep learning tools: An experimental study in medical imaging. *Multimedia Tools and Applications*, *81*(10), 13289–13317. https://doi.org/10.1007/s11042-021-10942-9

Alzubaidi, L., Fadhel, M. A., Oleiwi, S. R., Al-Shamma, O., & Zhang, J. (2020). DFU_QUTNet: Diabetic foot ulcer classification using novel deep convolutional neural network. *Multimedia Tools and Applications*, *79*(21), 15655–15677. https://doi.org/10.1007/s11042-019-07820-w

American Diabetes Association. (n.d.). *Diagnostic | ADA*. Retrieved December 4, 2022, from https://diabetes.org/diagnostico

Carter, J. A., Long, C. S., Smith, B. P., Smith, T. L., & Donati, G. L. (2019). Combining elemental analysis of toenails and machine learning techniques as a non-invasive diagnostic tool for the robust classification of type-2 diabetes. *Expert Systems with Applications*, *115*, 245–255. https://doi.org/10.1016/j.eswa.2018.08.002

Cruz-Vega, I., Hernandez-Contreras, D., Peregrina-Barreto, H., Rangel-Magdaleno, J. de J., & Ramirez-Cortes, J. M. (2020). Deep Learning Classification for Diabetic Foot Thermograms. *Sensors (Basel, Switzerland)*, *20*(6), 1762. https://doi.org/10.3390/s20061762

Diabetic foot ulcer (DFU). (n.d.). Retrieved March 3, 2023, from https://www.kaggle.com/datasets/laithjj/diabetic-foot-ulcer-dfu

Fregoso-Aparicio, L., Noguez, J., Montesinos, L., & García-García, J. A. (2021). Machine learning and deep learning predictive models for type 2 diabetes: A systematic review. *Diabetology & Metabolic Syndrome*, *13*(1), 148. https://doi.org/10.1186/s13098-021-00767-9

Goyal, M., Reeves, N. D., Davison, A. K., Rajbhandari, S., Spragg, J., & Yap, M. H. (2020). DFUNet: Convolutional Neural Networks for Diabetic Foot Ulcer Classification. *IEEE Transactions on Emerging Topics in Computational Intelligence*, *4*(5), 728–739. https://doi.org/10.1109/TETCI.2018.2866254

Hacisoftaoglu, R. E., Karakaya, M., & Sallam, A. B. (2020). Deep learning frameworks for diabetic retinopathy detection with smartphone-based retinal imaging systems. *Pattern Recognition Letters*, *135*, 409–417. https://doi.org/10.1016/j.patrec.2020.04.009

Hossain, Md. B., Iqbal, S. M. H. S., Islam, Md. M., Akhtar, Md. N., & Sarker, I. H. (2022). Transfer learning with fine-tuned deep CNN ResNet50 model for classifying COVID-19 from chest X-ray images. *Informatics in Medicine Unlocked*, *30*, 100916. https://doi.org/10.1016/j.imu.2022.100916

INEGI. (2022). *Estadísticas a propósito del día mundial de la diabetes*. https://www.inegi.org.mx/contenidos/saladeprensa/aproposito/2022/EAP_DIABETES2022.pdf

Ioffe, S., & Szegedy, C. (2015). *Batch Normalization: Accelerating Deep Network Training by Reducing Internal Covariate Shift* (arXiv:1502.03167). arXiv. https://doi.org/10.48550/arXiv.1502.03167

ISSN 2414-4924

Jain, P., Joshi, A. M., Agrawal, N., & Mohanty, S. (2020, January 24). *iGLU 2.0: A new non-invasive, accurate serum glucometer for smart healthcare*. ArXiv.Org. https://doi.org/10.1109/TCE.2020.3011966

Jiang, Z.-P., Liu, Y.-Y., Shao, Z.-E., & Huang, K.-W. (2021). An Improved VGG16 Model for Pneumonia Image Classification. *Applied Sciences*, *11*(23), Article 23. https://doi.org/10.3390/app112311185

Kathamuthu, N. D., Subramaniam, S., Le, Q. H., Muthusamy, S., Panchal, H., Sundararajan, S. C. M., Alrubaie, A. J., & Zahra, M. M. A. (2023). A deep transfer learning-based convolution neural network model for COVID-19 detection using computed tomography scan images for medical applications. *Advances in Engineering Software*, *175*, 103317. https://doi.org/10.1016/j.advengsoft.2022.103317

Krizhevsky, A., Sutskever, I., & Hinton, G. E. (2012). ImageNet Classification with Deep Convolutional Neural Networks. *Advances in Neural Information Processing Systems*, *25*. https://proceedings.neurips.cc/paper/2012/hash/c399862d3b9d6b76c8436e924a68c45b-Abstract.html

Martínez Pérez, J. A., & Pérez Martin, P. S. (2023). La curva ROC. *Medicina de Familia. SEMERGEN*, *49*(1), 101821. https://doi.org/10.1016/j.semerg.2022.101821

Munadi, K., Saddami, K., Oktiana, M., Roslidar, R., Muchtar, K., Melinda, M., Muharar, R., Syukri, M., Abidin, T. F., & Arnia, F. (2022). A Deep Learning Method for Early Detection of Diabetic Foot Using Decision Fusion and Thermal Images. *Applied Sciences*, *12*(15), Article 15. https://doi.org/10.3390/app12157524

OMS. (n.d.). *HEARTS D: Diagnosis and management of type 2 diabetes*. Retrieved December 5, 2022, from https://www.who.int/publications-detail-redirect/who-ucn-ncd-20.1

Patel, B., & Priefer, R. (2021). Infections associated with diabetic-care devices. *Diabetes & Metabolic Syndrome: Clinical Research & Reviews*, *15*(2), 519–524. https://doi.org/10.1016/j.dsx.2021.02.023

Qiao, L., Zhu, Y., & Zhou, H. (2020). Diabetic Retinopathy Detection Using Prognosis of Microaneurysm and Early Diagnosis System for Non-Proliferative Diabetic Retinopathy Based on Deep Learning Algorithms. *IEEE Access*, *8*, 104292–104302. https://doi.org/10.1109/ACCESS.2020.2993937

Salud, S. de. (n.d.). *Diabetes Mellitus Tipo 2 Hospitalaria 2022*. gob.mx. Retrieved May 31, 2023, from http://www.gob.mx/salud/documentos/diabetes-mellitus-tipo-2-hospitalaria-2022

Sanchez-Brito, M., Vazquez-Zapien, G. J., Luna-Rosas, F. J., Mendoza-Gonzalez, R., Martinez-Romo, J. C., & Mata-Miranda, M. M. (2022). Attenuated total reflection FTIR dataset for identification of type 2 diabetes using saliva. *Computational and Structural Biotechnology Journal*, *20*, 4542–4548. https://doi.org/10.1016/j.csbj.2022.08.038

Shukla, R., & Tiwari, A. (2022). Masked Face Recognition Using MobileNet V2 with Transfer Learning. *Computer Systems Science and Engineering*, *45*(1), 293–309. https://doi.org/10.32604/csse.2023.027986

Silva, K. D., Enticott, J., Barton, C., Forbes, A., Saha, S., & Nikam, R. (2021). Use and performance of machine learning models for type 2 diabetes prediction in clinical and community care settings: Protocol for a systematic review and meta-analysis of predictive modeling studies. *DIGITAL HEALTH*, *7*, 20552076211047390. https://doi.org/10.1177/20552076211047390

Tang, Y., Gao, R., Lee, H. H., Wells, Q. S., Spann, A., Terry, J. G., Carr, J. J., Huo, Y., Bao, S., & Landman, B. A. (2020). Prediction of Type II Diabetes Onset with Computed Tomography and Electronic Medical Records. In: Syeda-Mahmood, T., *et al*. Multimodal Learning for Clinical Decision Support and Clinical Image-Based Procedures. CLIP ML-CDS 2020 2020. Lecture Notes in Computer Science(), vol 12445. Springer, Cham. https://doi.org/10.1007/978-3-030-60946-7_2

Vanacore, A., Pellegrino, M. S., & Ciardiello, A. (2022). Fair evaluation of classifier predictive performance based on binary confusion matrix. *Computational Statistics*. https://doi.org/10.1007/s00180-022-01301-9

ISSN 2414-4924

Wang, K., Liu, M., Hao, X., & Xing, X. (2017). Decision-Level Fusion Method Based on Deep Learning. In J. Zhou, Y. Wang, Z. Sun, Y. Xu, L. Shen, J. Feng, S. Shan, Y. Qiao, Z. Guo, & S. Yu (Eds.), *Biometric Recognition* (pp. 673–682). Springer International Publishing. https://doi.org/10.1007/978-3-319-69923-3_72

WHO Library Cataloguing-in-Publication Data. (n.d.). *Diabetes*. Retrieved December 5, 2022, from https://www.who.int/news-room/fact-sheets/detail/diabetes

Xu, Y., Han, K., Zhou, Y., Wu, J., Xie, X., & Xiang, W. (2022). Classification of Diabetic Foot Ulcers Using Class Knowledge Banks. *Frontiers in Bioengineering and Biotechnology*, *9*. https://www.frontiersin.org/articles/10.3389/fbioe.2021.811028

Yap, M. H., Hachiuma, R., Alavi, A., Brüngel, R., Cassidy, B., Goyal, M., Zhu, H., Rückert, J., Olshansky, M., Huang, X., Saito, H., Hassanpour, S., Friedrich, C. M., Ascher, D. B., Song, A., Kajita, H., Gillespie, D., Reeves, N. D., Pappachan, J. M., … Frank, E. (2021). Deep learning in diabetic foot ulcers detection: A comprehensive evaluation. *Computers in Biology and Medicine*, *135*, 104596. https://doi.org/10.1016/j.compbiomed.2021.104596

Zhang, L., Wang, Y., Niu, M., Wang, C., & Wang, Z. (2021). Nonlaboratory-Based Risk Assessment Model For Type 2 Diabetes Mellitus Screening in Chinese Rural Population: A Joint Bagging-Boosting Model. *IEEE Journal of Biomedical and Health Informatics*, *25*(10), 4005–4016. https://doi.org/10.1109/JBHI.2021.3077114

ISSN 2414-4924

Article **ECORFAN Journal-Democratic Republic of Congo**
June, 2023 Vol.9 No.16 22-31

Detection of internal corrosion by long-pulse thermography and digital image processing

Detección de corrosión interna mediante termografía de pulso largo y procesamiento digital de imágenes

CASTILLO-VALDEZ, Georgina†*, LARIA-MENCHACA, Julio, GÓMEZ-CARPIZO, Santiago and SANDOVAL-SÁNCHEZ, Juan Antonio

Ingeniería en Tecnologías de la Información, Universidad Politécnica de Altamira. Nuevo Libramiento Altamira Km. 3, Santa Amalia, Altamira, Tamaulipas. C.P. 89602

ID 1st Author: *Georgina, Castillo-Valdez* / **ORC ID**: 0000-0001-7326-251X, **CVU CONAHCYT ID**: 164590

ID 1st Co-author: *Julio, Laria-Menchac*a / **ORC ID**: 0000-0001-5641-8535, **CVU CONAHCYT ID**: 123349

ID 2nd Co-author: *Santiago, Gómez-Carpizo* / **ORC ID**: 0000-0001-7714-2144, **CVU CONAHCYT ID**: 173219

ID 3rd Co-author: *Juan Antonio, Sandoval-Sánchez* / **ORC ID**: 0000-0003-2329-2440, **CVU CONAHCYT ID**: 727075

DOI: 10.35429/EJDRC.2023.16.9.22.31 Received March 10, 2023; Accepted June 30, 2023

Abstract

This paper addresses the problem of internal pitting corrosion in metals. The approach to solving this problem is carried out by means of long-pulse thermography (step heating) and digital image processing, using the median filter in the pre-processing and the Fourier transform in the processing. The long pulse thermography technique is an excellent way of detecting corrosion in metals. According to the state of the art, most of the works reviewed detect only the presence of external corrosion. In the experiments plates of different thickness were evaluated, one of 2 mm and another of 8 mm; this is another point in favor since most of the reviewed articles only focus on a single sample. In the development of this project, the following lines of research have been identified: implementation of new digital image processing methods, improvement of the thermography technique using other energy sources to heat the plates in a shorter time, exploring other functions of image processing in programming languages, carrying out tests with plates of different thickness and size, measuring the percentage of corrosion.

Infrared thermography, Long pulse thermography, Digital image processing

Resumen

En este trabajo se aborda el problema de la corrosión interna por picadura en metales. El enfoque de solución de este problema se plantea mediante termografía de pulso largo (step heating) y procesamiento digital de imágenes, utilizando en el preprocesamiento el filtro de mediana y en el procesamiento la transformada de Fourier. La técnica de termografía de pulso largo es una excelente forma de detección de corrosión en metales. De acuerdo al estado del arte, la mayoría de los trabajos revisados detectan sólo la presencia de corrosión externa. En los experimentos se evaluaron placas de diferente espesor, una de 2 milímetros y otra de 8 milímetros; este es otro punto a favor ya que en los artículos revisados la mayoría sólo se enfocan en una sola muestra. En el desarrollo de este proyecto se han identificado las siguientes líneas de investigación: implementación de nuevos métodos de procesamiento digital de imágenes, mejorar la técnica de termografía utilizando otras fuentes de energía para calentamiento de las placas en un menor tiempo, explorar otras funciones de procesamiento de imágenes en lenguajes de programación, realizar pruebas con placas de diferente espesor y tamaño, medir el porcentaje de corrosión.

Termografía infrarroja, Termografía de pulso largo, Procesamiento digital de imágenes

Citation: CASTILLO-VALDEZ, Georgina, LARIA-MENCHACA, Julio, GÓMEZ-CARPIZO, Santiago and SANDOVAL-SÁNCHEZ, Juan Antonio. Detection of internal corrosion by long-pulse thermography and digital image processing**.** ECORFAN Journal-Democratic Republic of Congo. 2023, 9-16: 22-31

* Correspondence to Author (e-mail: ccutietorres@gmail.com)
† Researcher contributing first author.

Introduction

Infrared thermography has evolved and is now widely accepted as a condition monitoring tool, where temperature is measured without contact (Talai *et al.*, 2016).

Corrosion detection is one of the main fields covered by Non Destructive Testing and Evaluation techniques in recent years and is the main problem for industries such as marine, petrochemical, aerospace, energy, automotive and others. There are different forms of corrosion in metals that could cause an unexpected or premature failure in the structure or component (Cadelano *et al*., 2016). For example, if a pipe or pipeline has a defect caused by corrosion, this can lead to leakage of the transported material, which would imply economic loss, environmental pollution and an area of risk for people nearby (Laaidi *et al*., 2011).

The hazardous condition of a corroded metal installation is difficult to assess by visual inspection, especially if it is an internal defect. The existence of corrosion can lead to accidents that have terrible technical, economic, environmental and social consequences (El-Amiri *et al*., 2017).

Thanks to significant improvements of the thermographic camera in the last twenty years, it has been possible to detect small cracks using an energy source with low frequency or short duration pulses (Shepard *et al*., 2004).

In this paper we will work with long pulse thermography (step heating), which has been successfully applied to evaluate defects in materials, achieving good efficiency (Kamińska *et al*., 2019).

Problem

Corrosion causes large economic losses in various industrial sectors, from infrastructure and transportation to production and manufacturing. A study conducted in the United States of America indicates that the annual direct cost related to corrosion is about $276 billion (Koch *et al*., 2010) representing approximately 3.1% of that nation's gross domestic product.

Globally, the direct cost of corrosion in countries is estimated to be between 3% and 4% of each country's gross domestic product (He *et al*., 2012).

Due to the constant maintenance of steel structures, the costs of corrosion are high. It is estimated that 20% of the steel consumed in Mexico is used to replace the material lost through corrosion (Corrosion, n.d.). In terms of safety, there are also costs due to accidents caused by corroded structures. In industries, it can cause temporary interruption of production, which represents large losses for companies.

This corrosion problem needs to be addressed by early detection.

In the following classical corrosion model, the factor known as general sensitivity to material loss is defined, which means that for every 1% increase in temperature in a corroded area, there is a 1% loss of material when t→∞.

$$\frac{\Delta L/L}{\Delta T/T} \approx 1 \quad (1)$$

Where $\Delta L/L$ is the loss of material and ΔT/T is the relative temperature which increases (Doshvarpassand *et a*l., 2019).

Justification

Inspection is an important part of many maintenance processes to maintain the safety of system components (Gao *et al*., 2014) and thus the integrity of the personnel working in each area.

It is important to detect defects in equipment in industries, in order to prevent unwanted accidents, to avoid leakage into the environment and to maintain the operational limits of the system components (Gherghinescu *et al*., 2013).

The present research is carried out for the timely detection of corrosion in industries or companies, in this way accidents can be avoided and acted upon in advance. It should be noted that the type of corrosion to be studied is pitting and internal corrosion in A36 carbon steel. The long pulse thermography technique will be implemented only at laboratory level.

ISSN 2414-4924

Related work

The works related to the topic addressed in this article are the following:

In (Shen & Li, 2007), the results show that infrared thermography is a reliable non-destructive method for the detection of defects produced by corrosion and erosion flow in a high temperature pipeline. The disadvantage of this method is the need to heat the pipes to change the temperature.

The authors (Wallbrink *et al*., 2007) present a quantitative estimation of defect size and depth using lock-in thermography on a 10 mm thick steel plate. With an excitation frequency of 0.02 Hz, the best thermal contrasts are found for the range of defects considered.

In this work (Marinetti & Vavilov, 2010), defects were simulated and material loss was modelled using the inversion formulae for both flash and square-pulse heating.

In (Liu *et al*., 2012) pulsed thermography is considered to rapidly quantify pitting corrosion in a pipe. A thermographic image processing procedure is proposed to extract corrosion information with phase congruency measurement and local binary fitting. The second principal component shows a good linear relationship with pipe metal loss.

In this paper (Vavilov e*t al*., 2013), hidden corrosion is detected in 1 to 2 mm thick steel containers that are used as temporary storage of radioactive waste.

(Xu *et al*., 2016), pulsed Eddy current thermography in combination with Principal Component Analysis provides an effective way to detect hidden defects in corroded steel bar. Step heating thermography was also used in the experiments.

In the article (Cadelano *et al*., 2016), infrared thermography was applied to detect corrosion in a real pipe segment with hot water inside the pipe at more than 90°C. The results show that the presence of water is better and can be considered as active thermography analysis.

(Li *et al*., 2017), this paper proposes a strategy to execute pre-processing and post-processing for surface defect detection based on the Eddy current pulsed thermography method. For preprocessing, it is used: Reconstruction of thermographic signals, Principal Component Analysis, Independent Component Analysis; for postprocessing, iterative thresholding, Otsu's method, slice histogram and iterative fitting are used.

In (Yang *et al*., 2019) proposed a method based on the combination of thermal image sequence reconstruction and first-order differential processing, used for noise removal and contrast enhancement respectively.

In the paper (Da Silva *et al*., 2020), an active thermography algorithm capable of detecting defects in materials was developed, based on the techniques of thermographic signal reconstruction, thermal contrast and physical principles of heat transfer.

The authors (Simonov *et al*., 2020), made a cube with plates of 2, 4, 6 and 8 mm thick, on the inner sides were simulated defects of different sizes, the experiment consisted in heating each plate at the same time with two halogen lamps of 1000 Watts each, the captured thermographic images were processed by Principal Components and Fourier Transform, also used the signal-to-noise ratio.

In this article we will work with the long pulse thermography technique (step heating), as it is an excellent technique for detecting internal corrosion in metals and has not been widely used.

Methodology

The proposed approach consists of five stages, which are shown in Figure 1 and described as follows.

ISSN 2414-4924

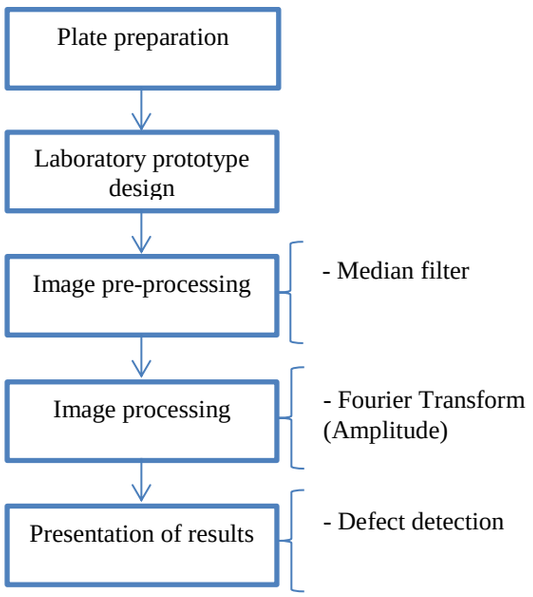

Figure 1 Solution approach for corrosion detection

Plate preparation

At this stage, A36 steel samples of size 15 centimetres wide by 15 centimetres long were prepared. Subsequently, holes of different diameters and depths were drilled in the central part of all the plates on the internal side, without going through the plate. Afterwards, salt water was added to the holes to cause corrosion, as well as residues of a corrosion rod, this process took about 3 weeks. As a next step, the plates were painted black on the outer side to improve the efficiency of the power source and reduce light reflection (Duan *et al.*, 2019).

The first plate, which will be referred to as plate 1, has a thickness of 2 millimetres and is shown in Figure 2.

Figure 2 (a) Plate 1 outer side, (b) Plate 1 inner side

Plates 2 and 3 have a thickness of 8 mm, as shown in Figures 3 and 4 respectively.

Figure 3 Plate 2 inner side

Figure 4 Plate 3 inner side

Laboratory prototype design

For the implementation of the prototype, two halogen lamps of 100 Watts each (Figure 5), a thermographic camera (Figure 6), the steel plates presented in the previous section and a computer were required. The thermographic camera was provided by the Polytechnic University of Altamira on loan.

Figure 5 100 Watt halogen lamps.

ISSN 2414-4924

Figure 6 Thermographic camera

A classic design of the prototype and the way images are acquired is shown in Figure 7. In this figure, the number 1 represents the energy source, in this case a 100 W halogen lamp. The images are acquired by reflection, i.e. the thermal imaging camera and the energy source are placed on the same side of the plate, transmission is when the thermal imaging camera and the energy source are on opposite sides of the plate. Reflection mode is used for internal defects and transmission mode for deep defects. Number 2 is the steel plate, number 4 is the computer on which the images are processed.

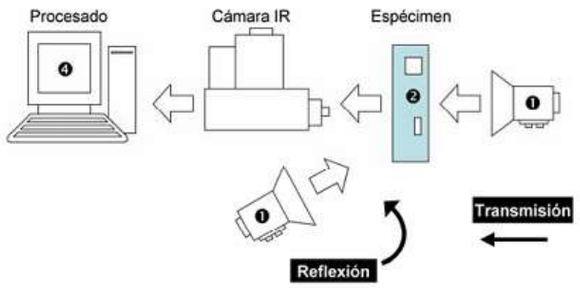

Figure 7 Prototype design *(Castanedo et al., 2014)*

Image pre-processing

Image pre-processing is very important, it is in charge of removing or filtering noise from the image so that it is ready for the next step, which is processing. In the experiments carried out, the median filter (Pratt, 1994) was used.

The median filter replaces each pixel of the image by the median of the pixels in the current filter region R, i.e.

$$I'(u,v) = mediana\{I(u+i, v+j)\} \quad (i,j) \in R \qquad (2)$$

The median of a set of 2n+1 values $A = \{a_0, \dots, a_{2n}\}$ can be defined as the central value a_n after arranging A in an ordered sequence, which is,

$$mediana(a_0, a_1, \dots a_{n-1}, \boldsymbol{a_n}, a_{n+1}, \dots, a_{2n}) = a_n \qquad (3)$$

Where $a_i \leq a_{i+1}$. Figure 8 demonstrates the calculation of the median size filter. 3 x 3.

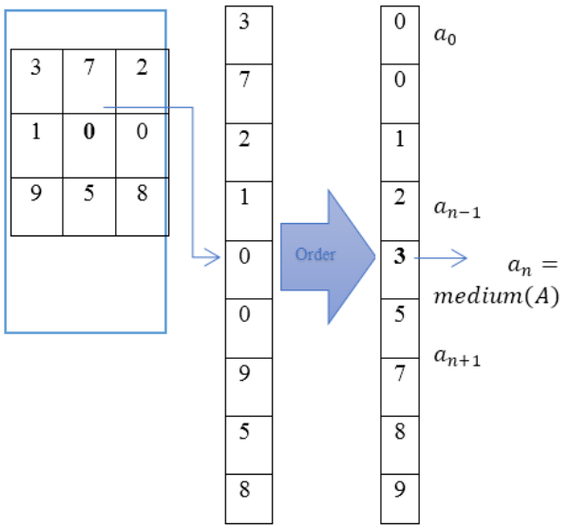

Figure 8 Median filter calculation

If the number of elements is even, then the median of the ordered sequence$A = (a_0, \dots, a_{2n-1})$ is defined as the arithmetical mean of the two central values a_{n-1} and a_n,

$$mediana(a_0, \dots \boldsymbol{a_{n-1}}, \boldsymbol{a_n}, \dots, a_{2n-1}) = \frac{a_{n-1}+a_n}{2} \qquad (3)$$

Image processing

The Fourier Transform, which is used to decompose an image into its sine and cosine components, was used for processing. The Fourier transform plays a fundamental role in a wide range of image processing applications, including enhancement, analysis, restoration and compression. The basic theory given by Fourier states that:

– Periodic functions can be represented by the sum of sine/cosine functions of different frequencies, multiplied by a different coefficient.

– Non-periodic functions can be represented as the integral of sine/cosine multiplied by the weight function.

ISSN 2414-4924

Digital images are used as input data. Thus, the discrete version of the Fourier Transform is used to convert a digital image into its frequency domain (Thanki & Kothari, 2018). This transform is known as Discrete Fourier Transform and given as:

$$F(u,v) = \frac{1}{MN}\sum_{x=0}^{M-1}\sum_{y=0}^{N-1} f(x,y)e^{-j2\pi(\frac{ux}{M}+\frac{vy}{N})} \quad (4)$$

where $u = 1, 0 \ldots M-1$ y $v = 0, 1, 2 \ldots N-1$.

Presentation of results

In this section, the identification or detection of defects, i.e. the identification of internal pitting corrosion, is carried out.

Experiment 1: Evaluation of plate 1

Objective: To identify internal pitting corrosion on the 2 mm thick plate.

Procedure: The plate was heated by reflection with the two 100 Watt halogen lamps for a period of 120 minutes at a distance of 10 centimetres on the outer side, the side with no holes or corrosion. Subsequently, a sequence of images was taken of the plate on the same side with the camera at a distance of 22 centimetres. The images were then taken from the camera and copied to the computer to make a selection of the images using the camera software and obtain those where, by adjusting the temperature, the defects can be seen. The selected images were then preprocessed and processed in the IR View software, which is free and open source, developed in Matlab by Laval University. The median filter was chosen for the pre-processing and the Fourier transform by amplitude for the processing.

Results

The chosen thermographic image of plate 1 is shown in Figure 9. The result of the image using the median filter can be seen in Figure 10.

Figure 11 shows plate 1 when using the amplitude Fourier transform.

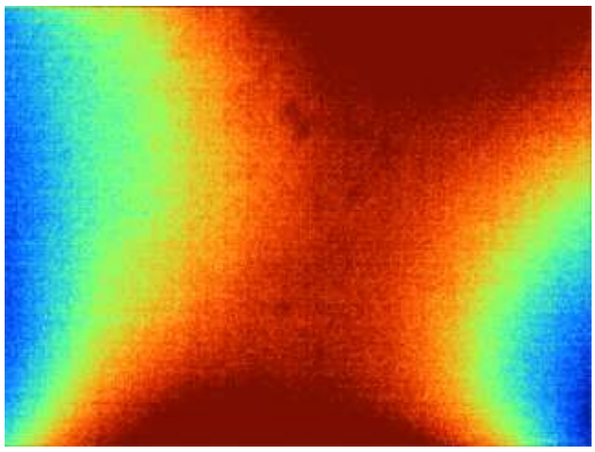

Figure 9 Thermographic image of plate 1

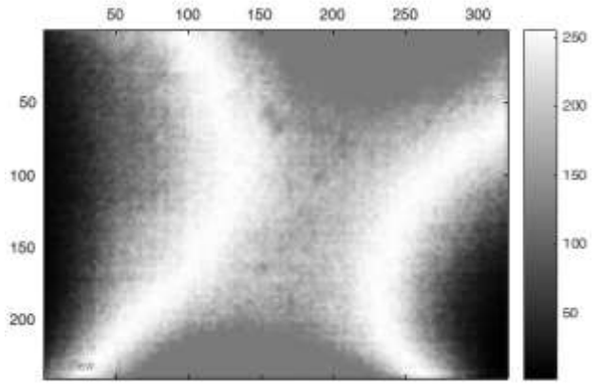

Figure 10 Plate 1 with median filter

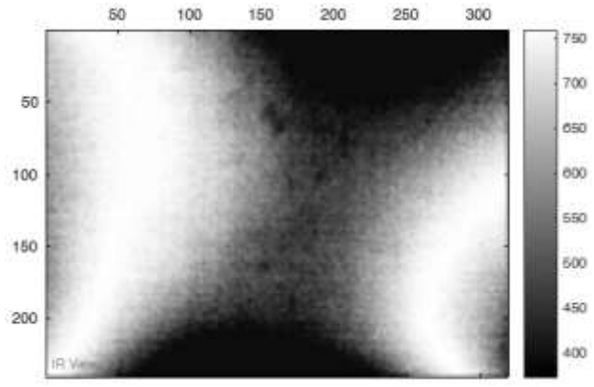

Figure 11 Amplitude Fourier Transform Plate 1

Experiment 2: Evaluation of plate 2

Aim: To find internal corrosion in plate 2 of 8 mm thickness.

Procedure: The power source was provided by two halogen lamps, placed 10 centimetres from the plate for 120 minutes. Several thermographic images were taken at a distance of 24 centimetres from the plate, a representative image was selected to apply the median filter and Fourier Transform by amplitude.

ISSN 2414-4924

Results

Figure 12 shows the thermographic image of plate 2.

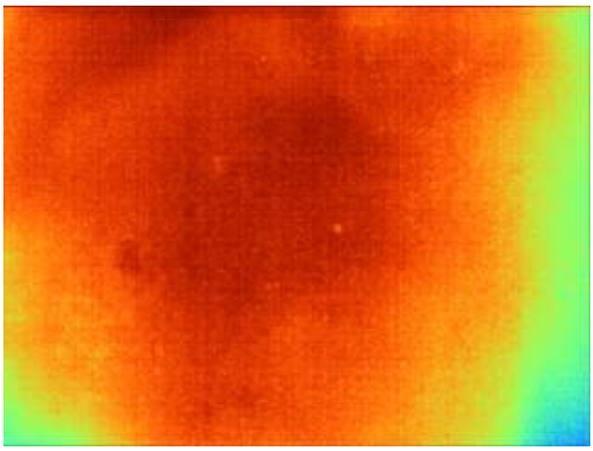

Figure 12 Thermographic image of plate 2

The thermographic image with the median filter is shown in Figure 13 and the applied Fourier transform is shown in Figure 14.

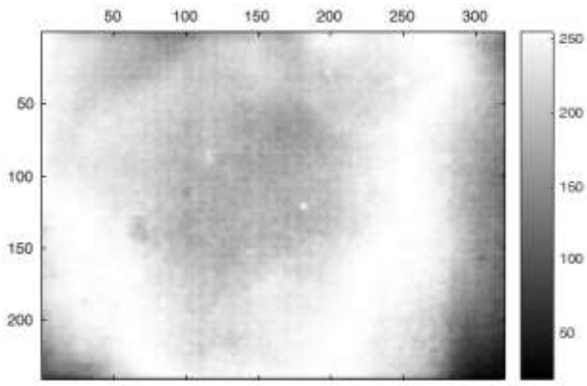

Figure 13 Plate 2 with median filter

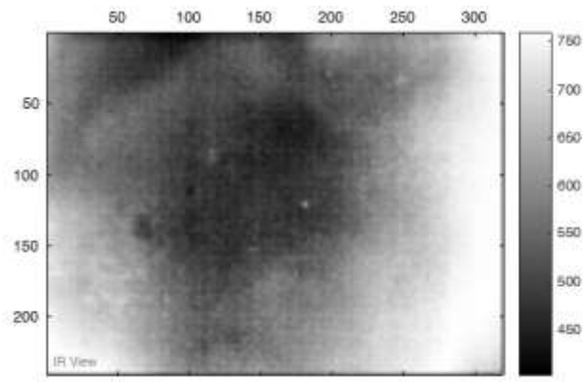

Figure 14 Plate 2 with amplitude Fourier transform.

Experiment 3: Plate evaluation 3

Objective: To detect internal corrosion in the 8 millimetre plate 3.

Procedure: Power was supplied to the plate with 100 W halogen lamps for 120 minutes at a distance of 10 centimetres, thermographic images were taken with the camera at a distance of 25 centimetres. The best image was considered and the median and amplitude Fourier transform filter was applied.

Results

The thermographic image, pre-processed and processed, are shown in Figures 15, 16 and 17 respectively.

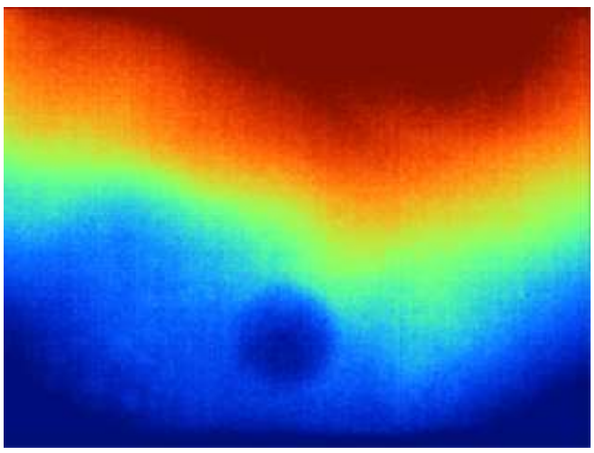

Figure 15 Thermographic image of plate 3

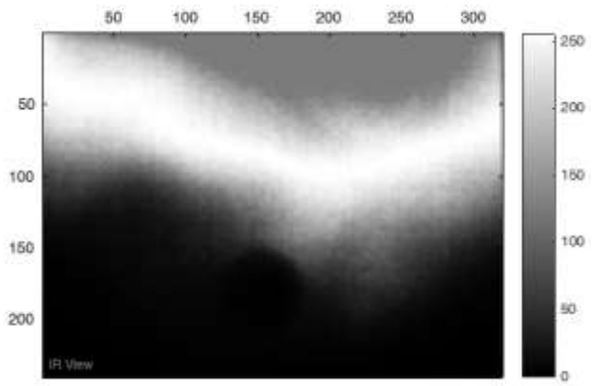

Figure 16 Image with median filter

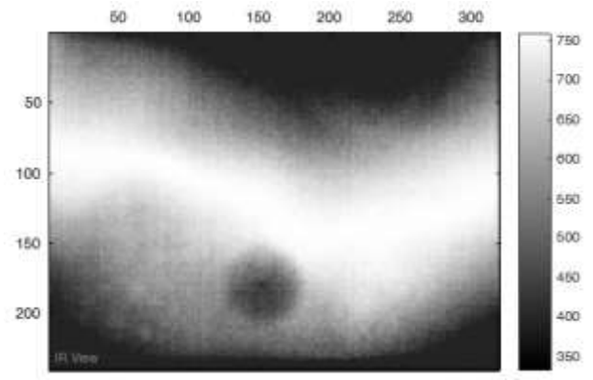

Figura 16 Fourier Transform Imaging

ISSN 2414-4924

Acknowledgements

My special gratitude to Dr. Clemente Ibarra for helping me to arrange the research stay, for sharing his knowledge, observations and subject material with me. Thanks to Laval University for allowing me to carry out the stay in their facilities, for the facilities granted such as access to books and articles from their databases, access to conferences.

I am grateful for the facilities provided by the Polytechnic University of Altamira to study this PhD and for the support with the loan of the thermographic camera.

Funding

I am grateful for the support granted by PRODEP through the official letter No. 511-6/18-8274 to carry out the PhD studies.

Conclusions

This work proposes a new technique for detecting internal pitting corrosion in metals, which can be implemented in real situations such as in a pipe or container transporting a substance.

The following lines of research were identified for future work:

– Implementation of new digital image processing methods. The concern arises to explore and implement other image processing methods to improve the result of the processed image.

– Improve the thermography technique using other energy sources. Given that the source used is very low power, the aim is to improve this energy source in order to heat the plates in a shorter time.

– Explore processing functions in programming languages.

– Perform tests with plates of different thickness and size.

– Measure the percentage of corrosion. Find out how to measure the corrosion percentage.

References

Cadelano, G., Bortolin, A., Ferrarini, G., Molinas, B., Giantin, D., Zonta, P., & Bison, P. (2016). Corrosion Detection in Pipelines Using Infrared Thermography: Experiments and Data Processing Methods. *Journal of Nondestructive Evaluation*, *35*(3), 1–11. https://doi.org/10.1007/s10921-016-0365-5

Castanedo, C. I., González, D. A., Bendada, H., & Maldague, X. (2014). Análisis de imágenes en Termografía Infrarroja. *Laboratoire de Vision et Systèmes Numériques de l'Université Laval*, 5. http://vision.gel.ulaval.ca/~bendada/publications/Id593.pdf

Corrosión. (s/f). Recuperado el 27 de noviembre de 2017, de http://amegac.mx/amegac.html

Da Silva, W. F., Melo, R. A. C., Grosso, M., Pereira, G. R., & Riffel, D. B. (2020). Active Thermography Data-Processing Algorithm for Nondestructive Testing of Materials. *IEEE Access*, *8*, 175054–175062. https://doi.org/10.1109/access.2020.3025329

Doshvarpassand, S., Wu, C., & Wang, X. (2019). An overview of corrosion defect characterization using active infrared thermography. *Infrared Physics and Technology*, *96*(November 2018), 366–389. https://doi.org/10.1016/j.infrared.2018.12.006

Duan, Y., Liu, S., Hu, C., Hu, J., Zhang, H., Yan, Y., Tao, N., Zhang, C., Maldague, X., Fang, Q., Ibarra-Castanedo, C., Chen, D., Li, X., & Meng, J. (2019). Automated defect classification in infrared thermography based on a neural network. *NDT and E International*, *107*(November 2018), 102147. https://doi.org/10.1016/j.ndteint.2019.102147

El-Amiri, A., Saifi, A., Halloua, H., Obbadi, A., Errami, Y., Elhassnaoui, A., & Sahnoun, S. (2017). Detection of corrosion depth in bolts by thermographic model. *Procedia Structural Integrity*, *5*, 1065–1071. https://doi.org/10.1016/j.prostr.2017.07.078

Gao, C., Meeker, W. Q., & Mayton, D. (2014). Detecting cracks in aircraft engine fan blades using vibrothermography nondestructive evaluation. *Reliability Engineering and System Safety*, *131*, 229–235. https://doi.org/10.1016/j.ress.2014.05.009

Gherghinescu, S., Popescu, G., & Spiridon, I. (2013). ADVANCED IR-NDT METHODS FOR THERMAL BALANCES OF HYDROGEN ISOTOPE EXCHANGE COLUMN. *Progress of Cryogenics and Isotopes Separation*, *16*(1), 89–97.

He, Y., Tian, G., Zhang, H., Alamin, M., Simm, A., & Jackson, P. (2012). Steel corrosion characterization using pulsed eddy current systems. *IEEE Sensors Journal*, *12*(6), 2113–2120. https://doi.org/10.1109/JSEN.2012.2184280

Kamińska, P., Ziemkiewcz, J., Synaszko, P., & Dragan, K. (2019). Comparison of Pulse Thermography (PT) and Step Heating (SH) Thermography in Non-Destructive Testing of Unidirectional GFRP Composites. *Fatigue of Aircraft Structures*, *2019*(11), 87–102. https://doi.org/10.2478/fas-2019-0009

Koch, G. H., Brongers, M. P. H., Thompson, N. G., Virmani, Y. P., & Payer, J. H. (2010). Corrosion Costs and Preventive Strategies in the United States. *NACE International*, *NACE*, 10. https://www.nace.org/uploadedFiles/Publications/ccsupp.pdf

Laaidi, N., Belattar, S., & Elbaloutti, A. (2011). Pipeline corrosion, modeling and analysis. *Journal of Nondestructive Evaluation*, *30*(3), 158–163. https://doi.org/10.1007/s10921-011-0103-y

Li, X., Gao, B., Woo, W. L., Tian, G. Y., Qiu, X., & Gu, L. (2017). Quantitative Surface Crack Evaluation Based on Eddy Current Pulsed Thermography. *IEEE Sensors Journal*, *17*(2), 412–421. https://doi.org/10.1109/JSEN.2016.2625815

Liu, Z., Genest, M., & Krys, D. (2012). Processing thermography images for pitting corrosion quantification on small diameter ductile iron pipe. *NDT and E International*, *47*, 105–115. https://doi.org/10.1016/j.ndteint.2012.01.003

Marinetti, S., & Vavilov, V. (2010). IR thermographic detection and characterization of hidden corrosion in metals: General analysis. *Corrosion Science*, *52*(3), 865–872. https://doi.org/10.1016/j.corsci.2009.11.005

Pratt, W. K. (1994). Digital Image Processing. En *European Journal of Engineering Education* (Vol. 19, Número 3). https://doi.org/10.1080/03043799408928319

Shen, G., & Li, T. (2007). Infrared thermography for high-temperature pressure pipe. *Insight: Non-Destructive Testing and Condition Monitoring*, *49*(3), 151–153. https://doi.org/10.1784/insi.2007.49.3.151

Shepard, S. M., Ahmed, T., & Lhota, J. R. (2004). Experimental considerations in vibrothermography. *Proceedings of SPIE*, *5405*, 332–335. https://doi.org/10.1117/12.546599

Simonov, D., Vavilov, V., & Chulkov, A. (2020). Infrared thermographic detector of hidden corrosion. *Sensor Review*, *40*(3), 283–289. https://doi.org/10.1108/SR-12-2019-0322

Talai, S. M., Desai, D. A., & Heyns, P. S. (2016). Vibration characteristics measurement of beam-like structures using infrared thermography. *Infrared Physics and Technology*, *79*, 17–24. https://doi.org/10.1016/j.infrared.2016.09.003

Thanki, R. M., & Kothari, A. M. (2018). Digital image processing using SCILAB. En *Digital Image Processing using SCILAB*. https://doi.org/10.1007/978-3-319-89533-8

Vavilov, V. P., Nesteruk, D. A., Chulkov, A. O., & Shiryaev, V. V. (2013). An apparatus for the active thermal testing of corrosion in steel cylindrical containers and test results. *Russian Journal of Nondestructive Testing*, *49*(11), 619–624. https://doi.org/10.1134/S1061830913110089

Wallbrink, C., Wade, S. A., & Jones, R. (2007). The effect of size on the quantitative estimation of defect depth in steel structures using lock-in thermography. *Journal of Applied Physics*, *101*(10), 1–9. https://doi.org/10.1063/1.2732443

ISSN 2414-4924

Xu, C., Zhou, N., Xie, J., Gong, X., Chen, G., & Song, G. (2016). Investigation on eddy current pulsed thermography to detect hidden cracks on corroded metal surface. *NDT and E International*, *84*, 27–35. https://doi.org/10.1016/j.ndteint.2016.07.002

Yang, Z., Kou, G., Li, Y., Tian, G., Zhang, W., & Zhu, J. (2019). Inspection Detectability Improvement for Metal Defects Detected by Pulsed Infrared Thermography. *Photonic Sensors*, *9*(2), 142–150. https://doi.org/10.1007/s13320-019-0489-1

ISSN 2414-4924

Article **ECORFAN Journal-Democratic Republic of Congo**
June 2023 Vol.9 No.16 32-37

Implementation of Matlab communication and Allen Bradley PLC for control of the AMATROL JUPITER XL Robot

Implementación de comunicación Matlab y PLC Allen Bradley para control del Robot AMATROL JUPITER XL

HERNÁNDEZ-JIMÉNEZ, Samuel Abinadí†*, ORTIZ-VÁZQUEZ, Jonathan, ORTIZ-SIMÓN, José Luis and CRUZ-HERNÁNDEZ, Nicolás

Instituto Tecnológico de Nuevo Laredo, Reforma 2007 Sur. Colonia Fundadores. Nuevo Laredo Tamaulipas, México

ID 1st Author: *Samuel Abinadí, Hernández-Jiménez* / **ORC ID**: 0009-0007-9013-1985

ID 1st Co-author: *Jonathan, Ortiz Vázquez* / **ORC ID**: 0000-0003-1087-9306, **Researcher ID Thomson**: S-7037-2018, **CVU CONAHCYT ID**: 999613

ID 2nd Co-author: *José Luis, Ortiz-Simón* / **ORC ID**: 0000-0001-6548-3849, **CVU CONAHCYT ID**: 209883

ID 3rd Co-author: *Nicolás, Cruz-Hernández* / **ORC ID**: 0000-0002-9780-0666

DOI: 10.35429/EJDRC.2023.16.9.32.37 Received March 10, 2023; Accepted June 30, 2023

Abstract

The article introduces a method to enable a robot, the "AMATROL JUPITER XL," without relying on its conventional controllers. Instead, a Human-Machine Interface (HMI) is employed using Allen Bradley's "ControlLogix 5550" software. This setup combines the engineering program MATLAB (via the Simulink extension) to develop control block diagrams containing calculations for robot design and comprehension. A data read-write interface is implemented on an "Allen Bradley 1756-L1" PLC, along with the integration of an Open Platform Communication (OPC) platform using the "RSLinx Classic" software. This configuration empowers the user to manipulate trajectories and objectives using calculations that depict the kinematics and dynamics of the mentioned robot. Consequently, this setup offers a control option that enables direct application of theoretical mathematical principles to the design and control aspects of robotics, leading to enhanced understanding of these principles.

HMI, Control, Robotic

Resumen

En este artículo se presenta una forma de habilitar un robot "AMATROL JUPITER XL" sin la utilización de sus controladores convencionales. En su lugar se utiliza una Interfaz Hombre - Máquina (HMI) usando el software de la empresa Allen Bradley "Control Logix 5550" con una configuración que combina el programa de ingeniería MATLAB (mediante la extensión de simulink, en el que se desarrollan el diagrama de control por bloques de comando los cuales contienen los cálculos para el diseño y comprensión de un robot) y una interfaz de lecto-escritura de datos, aplicada en un PLC "Allen Bradley 1756-L1", con la implementación de una Plataforma de comunicación Abierta (OPC) haciendo uso de los software "RSLinx Classic" la cual permite al usuario poder manipular las trayectorias, y los objetivos, empleando cálculos que representan la cinemática y dinámica del mencionado robot. Todo esto provee una opción de control que permite al usuario una aplicación directa de los principios teóricos matemáticos del diseño y el control en la robótica, permitiendo una mayor comprensión de los mismos.

HMI, Control, Robótica

Citation: HERNÁNDEZ-JIMÉNEZ, Samuel Abinadí, ORTIZ-VÁZQUEZ, Jonathan, ORTIZ-SIMÓN, José Luis and CRUZ-HERNÁNDEZ, Nicolás. Implementation of Matlab communication and Allen Bradley PLC for control of the AMATROL JUPITER XL Robot. ECORFAN Journal-Democratic Republic of Congo. 2023, 9-16: 32-37

* Correspondence to Author (e-mail: s.abinadi.hernandez@gmail.com)
† Researcher contributing first author.

Introduction

Robotics is one of the most exciting branches of engineering, but also one of the most complex subjects for a student. Institutions acquire equipment and due to the complexity of the design the software and controller provided by the company itself; this implies the need to be trained in the electronics and software provided to manipulate the robot. The tasks for the robot applied to control, trajectory tracking and positioning, require the use of specialized hardware and different for each robot manufacturer in the industry that are generally incompatible with each other, representing high costs in hardware acquisition and training in case of not having this equipment for a specific robot. At the Institute we have an obsolete but very functional robot which is no longer supported by the company and we do not have software and certain hardware to manipulate it. In this article we present the way in which we achieved the communication with the robot using Matlab Simulink programming through the Allen Bradley PLC 1756-L1 to have a "home-made" alternative to achieve the control of the industrial robot ADEPTO of 4 degrees of freedom AMATROL JUPITER XL.

The system that has been designed allows us to dispense with the acquisition of software and hardware from the manufacturer and achieve the rehabilitation of the robot that have been discontinued, also allows the unification of multiple work units and create a general communication network, allowing the integration of different automated machines.

Electrical System

It is worth mentioning that, although this alternative presents the solution in the application of not using the usual controls, the A721 servo amplifier driver is still used to control the power of the motors used in the "AMATROL JUPITER XL" robot (Figure 1).

Figure 1 Amatrol Jupiter XL Robot

Table 1 shows the identification of each of the cables that communicate from the robot to the controller, as well as the controller and the encoders which are routed and connected to the PLC; the 24 connector pins are identified and described in Figure 2.

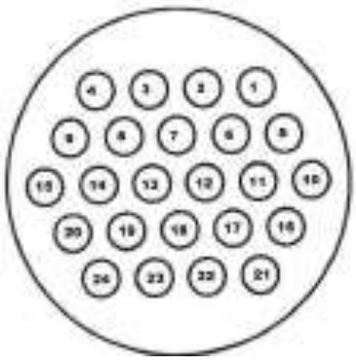

Figure 2 24-pin connector layout

Pin	Data	Pin	Data	Pin	Data
1	Engine 2 (+)	7	Motor 4 (+)	13	Tach 1 (+)
2	Engine 2 (-)	8	Engine 4 (-)	14	Tach 1 (-)
3	Engine 3 (+)	9	Tach 2 (+)	15	Tach 4 (+)
4	Engine 3 (-)	10	Tach 2 (-)	16	Tach 4 (-)
5	Engine 1 (+)	11	Tach 3 (+)	17-20	-
6	Engine 1 (-)	12	Tach 3 (-)	21-24	-

Table 1 Pin Identification

ISSN 2414-4924

An additional connection is necessary for the pneumatic drive area of the robot with the relation presented in table 2, which is a 16-pin connection as shown in figure 3 and will allow us to control the actuators from the PLC through the solenoid valves it contains, however, for the mentioned connection it is not necessary to take as a standard the pin relation presented in this article, since, being a created connection, it is left to the decision and definition of whoever uses it.

Pin	Data	Pin	Data	Pin	Data
1	RTN 1	7	RTN 4	13	-
2	Drive 1	8	Drive 4	14	-
3	RTN 2	9	Relay (-)	15	Relay (+)
4	Drive 2	10	-	16	Sensors (-)
5	RTN 3	11	Switch (+)	-	-
6	Drive 3	12	Switch (-)	-	-

Table 2 Identification of pins of the additional connection

Communication to PLC

For the communication of the robot to the PLC (figure 3) a 16-pin cable is used, whose connection is located in the controller and the 4 cables of 24 pins with output from the robot that correspond to the 4 encoders, making use of them, the connection to the PLC is made, the diagram of the controller cable pins is presented in figure 4, and the identification of them is presented in table 3.

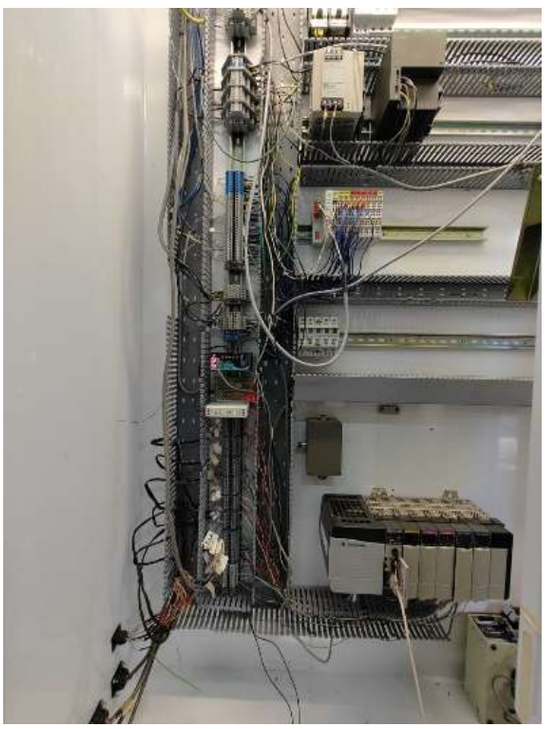

Figure 3 Cabinet with the connections between the robot and the PLC

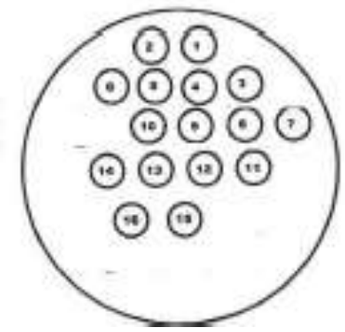

Figure 4 16-pin connector layout

Pin	Data	Pin	Data	Pin	Data
1	GND 12v	7	Valve 2	13	Tool 2
2	Tool	8	-	14	Valve 3
3	Tool 1	9	Valve 4	15	-
4	-	10	Valve 5	16	-
5	Tool 3	11	Valve 6	-	-
6	Valve 1	12	GND 24v	-	-

Table 3 Identification of the cable that communicates the controller with the PLC.

The "Allen Bradley PLC Control Logix 1756-A7 A series 7-slot Chassis" requires the integration of the modules described below:

"ControlLogix Controller and Memory Board 1756-L55" module, is used as a controller and non-volatile memory for storing virtual tags which are used for the operation of electrical components controlled from a computer machine.

The "ControlLogix High-Speed Counter Module (1756-HSC/A)" is used to count the pulses in the encoders, which occupy both input A and B of the counter, making the connection as shown in Figure 5. The relationship between these two channels determines whether it is positive or negative.

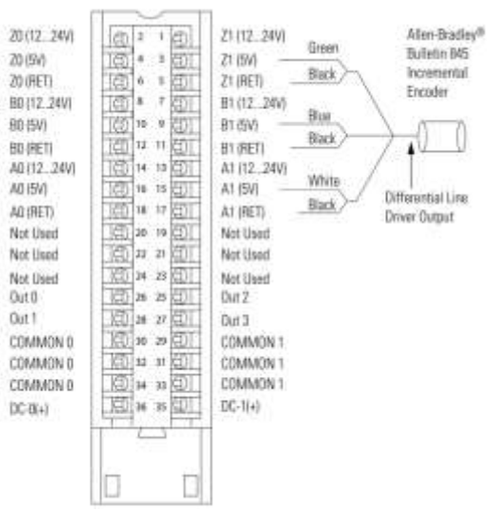

Figure 5 Encoder to PLC connection diagram

ISSN 2414-4924

The "ControlLogix I/O Module Analog Output (1756-OF8)" module is used to control the four motors of the "Amatrol Jupiter XL" robot, since this module manages the necessary voltages (positive or negative).

These ControlLogix output modules receive a signal from the A721 controller and process it internally through hardware and an ASIC (Application Specific Integrated Circuit) before sending the signal to the output device through the RTB as shown in Figure 6.

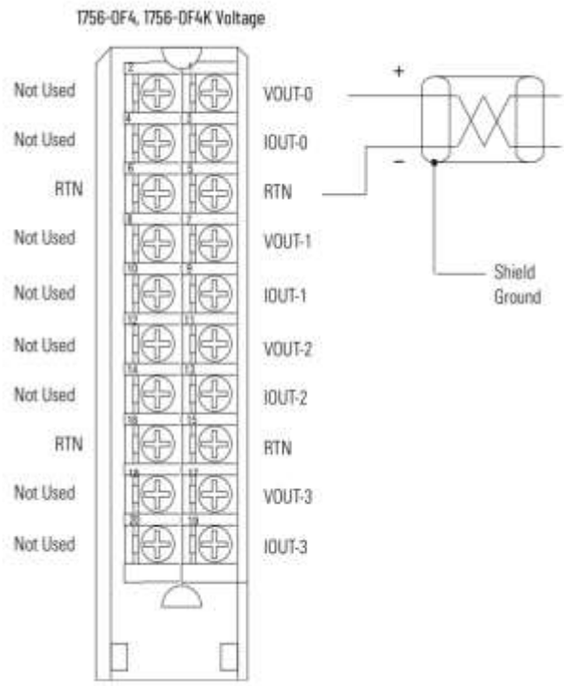

Figure 6 Wiring diagram for motor control.

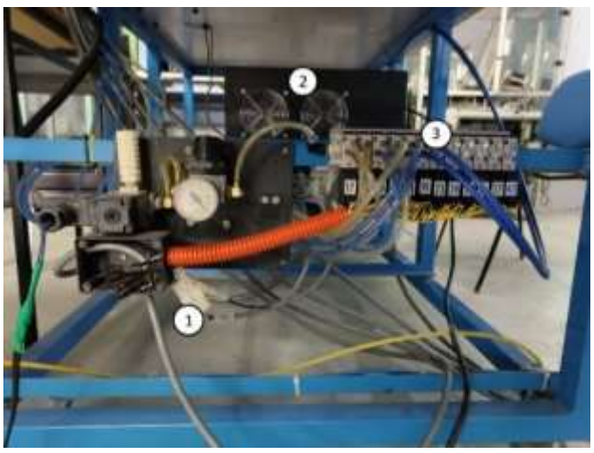

Figure 7 1) Connection 2) Servo controller. 3) Solenoid valves.

The "ControlLogix I/0 Module Digital Output (1756-OB8)" module is used to drive the solenoid valves (Figure 7) and the signals to the motor controller module using the diagram in Figure 8.

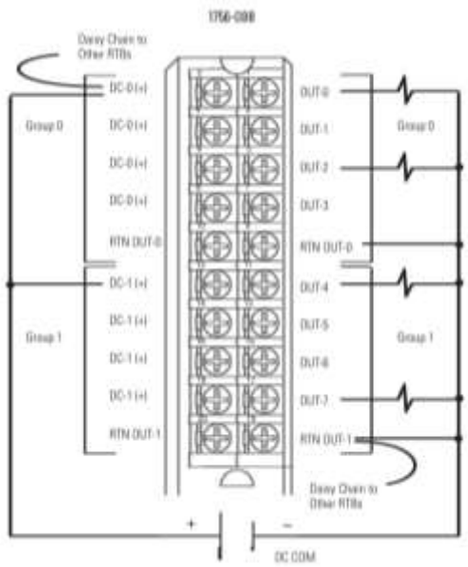

Figure 8 Connection diagram for valve control.

The Encoders use a cable with a 24-pin connector as shown in Figure 1, towards the PLC the classification identified in the cables is presented in Table 4.

Pin		Date	Pin	Date	Pin	Date
1		A	7	5v	13	-
2		$\overline{A}$	8	0v	14	-
3		B	9	-	15	-
4		$\overline{B}$	10	-	16	-
5		Z	11	-	17	-
6		$\overline{Z}$	12	-	18-24	-

Table 4 Identification of encoder cables

PLC-RSLogix Communication

Through the serial communication port a relationship is established between the PLC and the computer, using the RSLogix 5000 program the configurations for each of the modules that are used are established, and later, with the creation of a main program the labels for each of the outputs and inputs of the system are created and loaded to the PLC, this allows the user to have an almost instantaneous visualization of the data obtained from the encoders and sensors, likewise it allows the drive of the motors and therefore the manipulation of the trajectories (figure 9).

ISSN 2414-4924

The tags created in the main program that is loaded to the PLC are essential for communication from the MATLAB program because it allows the values to be modified in real time, with a slight delay of no more than 1s from the time it is modified until the robot responds.

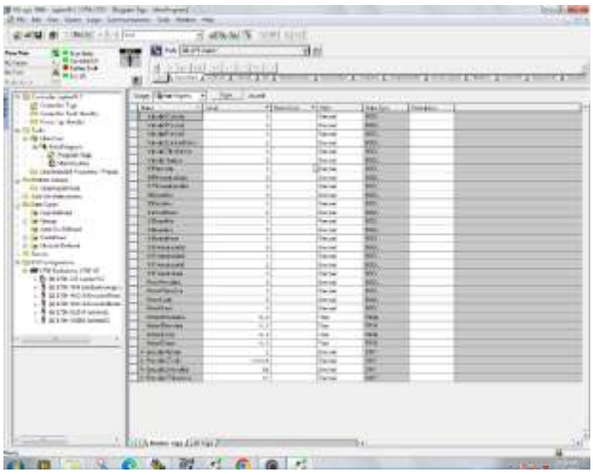

Figure 9 RSLogix 5000 software running with the tags; here we can see the information obtained from the tool's sensors reflected by the Boolean value 1

ControlLogix link to MATLAB

Using the programs "RsLinx Classic Gateway" and "DeviceNet - RSNetWork for DeviceNet" an OPC is built to allow the transfer of information between the PLC programs and the program to be used for the simulation and design of the robot trajectories, which in this particular case are RSLogix 5000 and MATLAB respectively, so that the values of the tags created can be modified, thus obtaining movement and manipulation of the physical system of the robot.

Control program in MATLAB

In order to obtain a precise movement of the robot using the MATLAB tool (SIMULINK), a virtual PID control system must be designed which allows the modification and correction of the positions and speeds required.

In the same way, the program displays data of analysis of the robotic system such as Position, Velocity, Angular velocity, Acceleration, etc.

The virtual system for the control of the robot requires for its operation data such as initial position or desired position (which are dictated by the user), and making use of mathematics; it uses operations such as inverse kinematics, direct kinematics, PID calculation (Proportional, Integral and Derivative), to define the voltage for the torque of the motors, find the position, regulate the speed and acceleration in the trajectory defined by values in radians.

Results

In the electrical part we found complete functionality of the electrical systems that allowed a correct communication to the PLC. This allows us to work successfully from the computer with a time lag of less than 1 second between the action requested in the computer and the action performed in the mechanical system of the robot.

From the communication with Matlab, the previous tests to the system mentioned in this article, which only requires the manipulation of a single value were successful, achieved movement in the robot from the MATLAB program, Figure 10 presents an example of the visualization of the communication.

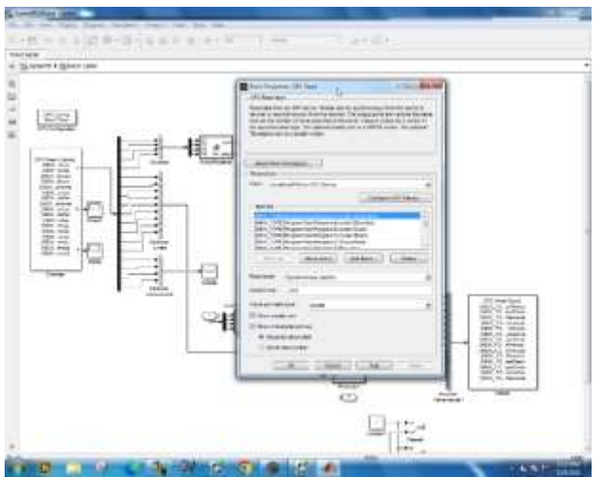

Figure 10 The labels created in a program must be able to be shared and visualized in MATLAB

ISSN 2414-4924

HERNÁNDEZ-JIMÉNEZ, Samuel Abinadí, ORTIZ-VÁZQUEZ, Jonathan, ORTIZ-SIMÓN, José Luis and CRUZ-HERNÁNDEZ, Nicolás. Implementation of Matlab communication and Allen Bradley PLC for control of the AMATROL JUPITER XL Robot. ECORFAN Journal-Democratic Republic of Congo. 2023

Conclusion

We know that the implementation of this control system for a robotic system is feasible, and useful for the academic area studying robotics, however, the complete control system employing PID back analysis by MATLAB is still under development with good expectations from the project.

References

Allen Bradley. (2009). *Datos de tags y E/S en los controladores Logix5000 publicación 1756-PM004C-ES-P-Octubre 2009.*

Allen Bradley. (2015). *Módulos de E/S analógicas ColtrolLogix publicación 1756-UM009-ES-P-Marzo 2015.*

Allen Bradley. (2015). *Módulos de E/S digitales ControlLogix publicación 1756-UM05H-ES-P-Mayo 2015.*

Allen Bradley. (2021). *Módulo contador de alta velocidad ControlLogix publicación 1756-UM007E-ES-P-Agosto 2021*.

Automática e instrumentación. (2021). *Mitsubishi Electric lanza el cobot Melfa Assista.* Obtenido de : https://www.automaticaeinstrumentacion.com/texto-diario/mostrar/2734545/mitsubishi-electric-lanza-cobot-melfa-assista el 7 de diciembre de 2022.

AUTYCOM. (2019). *Paneles SIMATIC HMI Comfort: eficiencia al más alto nivel*. Obtenido de : https://www.autycom.com/paneles-simatic-hmi-comfort-eficiencia-al-mas-alto-nivel/ el 7 de diciembre de 2022.

Casares, J. (15 de septiembre de 2015). *Historia de OPC*. Obtenido de: https://josecasares.com/historia-de-opc/ el 7 de diciembre de 2022.

Honeywell International INC. (2022). *OPC Server*. Obtenido de: https://www.matrikonopc.com/opc-server/ el 7 de diciembre de 2022.

La Vanguardia. (2022). *Robot Gargantua.* Obtenido de: https://www.lavanguardia.com/vida/junior-report/20220610/8330874/historia-robotica.html el 7 de diciembre de 2022.

MathWorks. (2014). *How to Create a GUI with GUIDE*. Obtenido de: https://la.mathworks.com/videos/creating-a-gui-with-guide-68979.html el 7 de diciembre de 2022.

MathWorks. (2021). *Simulink para el diseño basado en modelos*. Obtenido de: https://la.mathworks.com/products/simulink.html el 7 de diciembre de 2022.

Monsalvo, S. (2020). *Automa cavaliere.* Obtenido de: https://www.babelxxi.com/469-automa-cavaliere-leonardo-da-vinci/ el 7 de diciembre de 2022.

nunsys. (2021). *¿Qué es un SCADA?: Control de Supervisión y Adquisición de Datos*. Obtenido de: https://www.nunsys.com/scada/ el 7 de diciembre de 2022.

Programador click. (2021). *¿Quiere saber cómo configurar DCOM al utilizar el servidor OPC?* Obtenido de : https://programmerclick.com/article/54551648688/ el 7 de diciembre de 2022.

Sandiman. (2021). *Robots Manipuladores.* Obtenido de: https://sandiman.cl/area/robots-manipuladores/ el 7 de diciembre de 2022.

Sapiensman. (2010). *Soldadura robotica.* Obtenido de: http://www.sapiensman.com/tecnoficio/soldadura/soldadura_robotica.php el 7 de diciembre de 2022.

Thakur, D. (2011). *What is OLE (object linking and embedding)?* Obtenido de: https://ecomputernotes.com/visual-basic/basic-of-visual-basic/ole el 7 de diciembre de 2022.

TIBCO. (2021). *¿Qué es la integración basada en APIs?* Obtenido de: https://www.tibco.com/es/reference-center/what-is-api-led-integration el 7 de diciembre de 2022

TOSHIBA. (2012). *PLC.* Obtenido de : https://www.toshiba.com/tic/es/other-products/plcs el 7 de diciembre de 2022.

WESTAMP INC. (1988). *Instruction manual for the a722x series dc servo amplifier revision c. Santa Monica.*

ISSN 2414-4924

[Title in Times New Roman and Bold No. 14 in English and Spanish]

Surname (IN UPPERCASE), Name 1st Author†*, Surname (IN UPPERCASE), Name 1st Coauthor, Surname (IN UPPERCASE), Name 2nd Coauthor and Surname (IN UPPERCASE), Name 3rd Coauthor

Institutional Affiliation of Author including Dependency (No.10 Times New Roman and Italic)

International Identification of Science - Technology and Innovation

ID 1st Author: (ORC ID - Researcher ID Thomson, arXiv Author ID - PubMed Author ID - Open ID) and CVU 1st author: (Scholar-PNPC or SNI-CONAHCYT) (No.10 Times New Roman)

ID 1st Coauthor: ((ORC ID - Researcher ID Thomson, arXiv Author ID - PubMed Author ID - Open ID) and CVU 1st author: (Scholar-PNPC or SNI-CONAHCYT) (No.10 Times New Roman)

ID 2nd Coauthor: (ORC ID - Researcher ID Thomson, arXiv Author ID - PubMed Author ID - Open ID) and CVU 1st author: (Scholar-PNPC or SNI-CONAHCYT) (No.10 Times New Roman)

ID 3rd Coauthor: (ORC ID - Researcher ID Thomson, arXiv Author ID - PubMed Author ID - Open ID) and CVU 1st author: (Scholar-PNPC or SNI-CONAHCYT) (No.10 Times New Roman)

(Report Submission Date: Month, Day, and Year); Accepted (Insert date of Acceptance: Use Only ECORFAN)

Abstract (In English, 150-200 words)

Objectives
Methodology
Contribution

Abstract (In Spanish, 150-200 words)

Objectives
Methodology
Contribution

Keywords (In English)

Indicate 3 keywords in Times New Roman and Bold No. 10

Keywords (In Spanish)

Indicate 3 keywords in Times New Roman and Bold No. 10

Citation: Surname (IN UPPERCASE), Name 1st Author, Surname (IN UPPERCASE), Name 1st Coauthor, Surname (IN UPPERCASE), Name 2nd Coauthor and Surname (IN UPPERCASE), Name 3rd Coauthor. Paper Title. ECORFAN Journal-Democratic Republic of Congo. Year 1-1: 1-11 [Times New Roman No.10]

* Correspondence to Author (example@example.org)
† Researcher contributing as first author.

Introduction

Text in Times New Roman No.12, single space.

General explanation of the subject and explain why it is important.

What is your added value with respect to other techniques?

Clearly focus each of its features

Clearly explain the problem to be solved and the central hypothesis.

Explanation of sections Article.

Development of headings and subheadings of the article with subsequent numbers

[Title No.12 in Times New Roman, single spaced and bold]

Products in development No.12 Times New Roman, single spaced.

Including graphs, figures and tables-Editable

In the article content any graphic, table and figure should be editable formats that can change size, type and number of letter, for the purposes of edition, these must be high quality, not pixelated and should be noticeable even reducing image scale.

[Indicating the title at the bottom with No.10 and Times New Roman Bold]

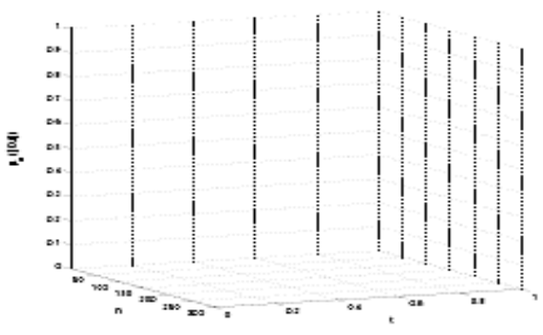

Graphic 1 Title and *Source (in italics)*

Should not be images-everything must be editable.

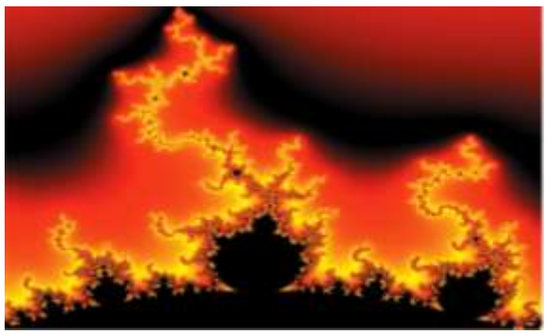

Figure 1 Title and *Source (in italics)*

Should not be images-everything must be editable.

Table 1 Title and *Source (in italics)*

Should not be images-everything must be editable.

Each article shall present separately in **3 folders**: a) Figures, b) Charts and c) Tables in .JPG format, indicating the number and sequential Bold Title.

For the use of equations, noted as follows:

$$Y_{ij} = \alpha + \sum_{h=1}^{r} \beta_h X_{hij} + u_j + e_{ij} \quad (1)$$

Must be editable and number aligned on the right side.

Methodology

Develop give the meaning of the variables in linear writing and important is the comparison of the used criteria.

Results

The results shall be by section of the article.

Annexes

Tables and adequate sources

Thanks

Indicate if they were financed by any institution, University or company.

Conclusions

Explain clearly the results and possibilities of improvement.

ISSN 2414-4924

References

Use APA system. Should not be numbered, nor with bullets, however if necessary numbering will be because reference or mention is made somewhere in the Article.

Use Roman Alphabet, all references you have used must be in the Roman Alphabet, even if you have quoted an Article, book in any of the official languages of the United Nations (English, French, German, Chinese, Russian, Portuguese, Italian, Spanish, Arabic), you must write the reference in Roman script and not in any of the official languages.

Technical Specifications

Each article must submit your dates into a Word document (.docx):

Journal Name
Article title
Abstract
Keywords
Article sections, for example:

1. *Introduction*
2. *Description of the method*
3. *Analysis from the regression demand curve*
4. *Results*
5. *Thanks*
6. *Conclusions*
7. *References*

Author Name (s)
Email Correspondence to Author
References

Intellectual Property Requirements for editing:

- Authentic Signature in Color of Originality Format Author and Coauthors
- Authentic Signature in Color of the Acceptance Format of Author and Coauthors
- Authentic Signature in Color of the Conflict of Interest Format of Author and Co-authors.

ISSN 2414-4924

Reservation to Editorial Policy

ECORFAN-Democratic Republic of Congo reserves the right to make editorial changes required to adapt the Articles to the Editorial Policy of the Journal. Once the Article is accepted in its final version, the Journal will send the author the proofs for review. ECORFAN® will only accept the correction of errata and errors or omissions arising from the editing process of the Journal, reserving in full the copyrights and content dissemination. No deletions, substitutions or additions that alter the formation of the Article will be accepted.

Code of Ethics - Good Practices and Declaration of Solution to Editorial Conflicts

Declaration of Originality and unpublished character of the Article, of Authors, on the obtaining of data and interpretation of results, Acknowledgments, Conflict of interests, Assignment of rights and Distribution

The ECORFAN-Mexico, S.C Management claims to Authors of Articles that its content must be original, unpublished and of Scientific, Technological and Innovation content to be submitted for evaluation.

The Authors signing the Article must be the same that have contributed to its conception, realization and development, as well as obtaining the data, interpreting the results, drafting and reviewing it. The Corresponding Author of the proposed Article will request the form that follows.

Article title:

– The sending of an Article to ECORFAN-Democratic Republic of Congo emanates the commitment of the author not to submit it simultaneously to the consideration of other series publications for it must complement the Format of Originality for its Article, unless it is rejected by the Arbitration Committee, it may be withdrawn.

– None of the data presented in this article has been plagiarized or invented. The original data are clearly distinguished from those already published. And it is known of the test in PLAGSCAN if a level of plagiarism is detected Positive will not proceed to arbitrate.

– References are cited on which the information contained in the Article is based, as well as theories and data from other previously published Articles.

– The authors sign the Format of Authorization for their Article to be disseminated by means that ECORFAN-Mexico, S.C. In its Holding Democratic Republic of Congo considers pertinent for disclosure and diffusion of its Article its Rights of Work.

– Consent has been obtained from those who have contributed unpublished data obtained through verbal or written communication, and such communication and Authorship are adequately identified.

– The Author and Co-Authors who sign this work have participated in its planning, design and execution, as well as in the interpretation of the results. They also critically reviewed the paper, approved its final version and agreed with its publication.

– No signature responsible for the work has been omitted and the criteria of Scientific Authorization are satisfied.

– The results of this Article have been interpreted objectively. Any results contrary to the point of view of those who sign are exposed and discussed in the Article.

Copyright and Access

The publication of this Article supposes the transfer of the copyright to ECORFAN-Mexico, SC in its Holding Democratic Republic of Congo for its ECORFAN-Democratic Republic of Congo, which reserves the right to distribute on the Web the published version of the Article and the making available of the Article in This format supposes for its Authors the fulfilment of what is established in the Law of Science and Technology of the United Mexican States, regarding the obligation to allow access to the results of Scientific Research.

Article Title:

Name and Surnames of the Contact Author and the Coauthors	Signature
1.	
2.	
3.	
4.	

Principles of Ethics and Declaration of Solution to Editorial Conflicts

Editor Responsibilities

The Publisher undertakes to guarantee the confidentiality of the evaluation process, it may not disclose to the Arbitrators the identity of the Authors, nor may it reveal the identity of the Arbitrators at any time.

The Editor assumes the responsibility to properly inform the Author of the stage of the editorial process in which the text is sent, as well as the resolutions of Double-Blind Review.

The Editor should evaluate manuscripts and their intellectual content without distinction of race, gender, sexual orientation, religious beliefs, ethnicity, nationality, or the political philosophy of the Authors.

The Editor and his editing team of ECORFAN® Holdings will not disclose any information about Articles submitted to anyone other than the corresponding Author.

The Editor should make fair and impartial decisions and ensure a fair Double-Blind Review.

Responsibilities of the Editorial Board

The description of the peer review processes is made known by the Editorial Board in order that the Authors know what the evaluation criteria are and will always be willing to justify any controversy in the evaluation process. In case of Plagiarism Detection to the Article the Committee notifies the Authors for Violation to the Right of Scientific, Technological and Innovation Authorization.

Responsibilities of the Arbitration Committee

The Arbitrators undertake to notify about any unethical conduct by the Authors and to indicate all the information that may be reason to reject the publication of the Articles. In addition, they must undertake to keep confidential information related to the Articles they evaluate.

Any manuscript received for your arbitration must be treated as confidential, should not be displayed or discussed with other experts, except with the permission of the Editor.

The Arbitrators must be conducted objectively, any personal criticism of the Author is inappropriate.

The Arbitrators must express their points of view with clarity and with valid arguments that contribute to the Scientific, Technological and Innovation of the Author.

The Arbitrators should not evaluate manuscripts in which they have conflicts of interest and have been notified to the Editor before submitting the Article for Double-Blind Review.

Responsibilities of the Authors

Authors must guarantee that their articles are the product of their original work and that the data has been obtained ethically.

Authors must ensure that they have not been previously published or that they are not considered in another serial publication.

Authors must strictly follow the rules for the publication of Defined Articles by the Editorial Board.

The authors have requested that the text in all its forms be an unethical editorial behavior and is unacceptable, consequently, any manuscript that incurs in plagiarism is eliminated and not considered for publication.

Authors should cite publications that have been influential in the nature of the Article submitted to arbitration.

Information services

Indexation - Bases and Repositories

RESEARCH GATE (Germany)
GOOGLE SCHOLAR (Citation indices-Google)
REDIB (Ibero-American Network of Innovation and Scientific Knowledge- CSIC)
MENDELEY (Bibliographic References Manager)

Publishing Services

Citation and Index Identification H
Management of Originality Format and Authorization
Testing Article with PLAGSCAN
Article Evaluation
Certificate of Double-Blind Review
Article Edition
Web layout
Indexing and Repository
ArticleTranslation
Article Publication
Certificate of Article
Service Billing

Editorial Policy and Management

31 Kinshasa 6593 – Republique Démocratique du Congo. Phones: +52 1 55 6159 2296, +52 1 55 1260 0355, +52 1 55 6034 9181; Email: contact@ecorfan.org www.ecorfan.org

ECORFAN Journal-Democratic Republic of Congo

2414 4924
ISSN 2414 - 4924

www.ecorfan.org